blue at pH 0.3–1.0 or with toluidine blue. Mast cells that contained esterase activities were identified as described[31]. Peritoneal mast cells were identified as cells that were positive for both FcεRI and c-Kit using flow cytometry (FACScan, Beeton Dickinson, San Jose, CA) as described[58].

Counting of tissue mast cells. Tissue mast cells were counted under a microscope and the data presented as the number of mast cells in each tissue unit. Each ear dermis unit was a 5-mm ear section along the cartilage; ear thickness was almost identical in all samples. In the back dermis, mast cells were counted and data presented as the number of mast cells per ten high power (×100) fields. Each gastric unit was the entire area of one sagittal section; both the forestomach and glandular stomach were included. The areas of gastric sections examined were almost identical in $PI3K^{+/+}$, $PI3K^{+/-}$ and $PI3K^{-/-}$ mice. Each intestinal mast cell unit was six horizontal sections of each portion, namely jejunum, ileum and colon.

IgE-dependent passive systemic anaphylaxis. Mice were intraveneously injected with monoclonal anti–TNP IgE (20 μg/mouse), a gift of H. Karasuyama (Tokyo Medical and Dental University), 1 day before antigen challenge. After 24 h, IgE-treated mice were intraveneously challenged with 1 mg of polyvalent trinitrophenyl–bovine serum albumin (TNP-BSA, LSL, Japan) in 100 μl of PBS–0.5% Evans blue dye (Sigma, St. Louis, MO). Extravasation of Evans blue in the ear and shock-induced death within 30 min of challenge were monitored. To determine the degree of histamine release in response to PSA, IgE-sensitized mice (2 μg per mouse) were challenged by intravenous injection of 500 μg of TNP-BSA for 3 min. Mice were then immediately killed and blood collected by cardiac puncture. Serum histamine concentrations were determined with a competitive histamine immunoassay kit (IBL, Hamburg, Germany).

Degranulation assay. The degree of degranulation was examined by measuring the release of β-hexosaminidase. $PI3K^{+/+}$ and $PI3K^{-/-}$ BMMCs were sensitized for 4 h with anti–TNP IgE (1 μg/ml) in CM without IL-3. To measure β-hexosaminidase release, sensitized cells were stimulated with TNP-BSA (10 ng/ml) or thapsigargin (1 μM, Sigma) for 20 min in Tyrode's buffer (10 mM HEPES buffer at pH 7.4, 130 mM NaCl, 5 mM KCl, 1.4 mM $CaCl_2$, 1 mM $MgCl_2$, 5.6 mM glucose and 0.1% BSA). Samples were centrifuged and supernatants collected. Cell pellets were solubilized with 0.5% Triton X-100 in Tyrode's buffer. The enzymatic activities of β-hexosaminidase in supernatants and cell lysates were measured with *p*-nitrophenyl N-acetyl-β-D-glucosaminide (Sigma) in 0.1 M sodium citrate (pH 4.5) for 60 min at 37 °C. The reaction was stopped by the addition of 0.2 M glycine (pH 10.7). Production of *p*-nitrophenol was detected by absorbance at 405 nm. The extent of degranulation was calculated by dividing *p*-nitrophenol absorbance in the supernatant by the sum of absorbance in the supernatant and cell lysate.

Bone marrow transplantation and reconstitution of BMMCs in $PI3K^{-/-}$ mice. Femoral bone marrow cells (1×10^7/mouse) from BALB/c mice were intraveneously injected into sublethally irradiated (4 Gy) $PI3K^{-/-}$ mice. BMMCs were obtained by culturing isolated progenitors from the femurs of BALB/c or $PI3K^{-/-}$ mice for 4–8 weeks in IL-3–supplemented medium. BMMCs (5×10^6/mouse) were then intraveneously injected into $PI3K^{-/-}$ mice. Eleven to twelve weeks after bone marrow transplantation or BMMC reconstitution, tissue specimens were prepared and the presence of mast cells in the gastrointestinal tracts examined. BMMCs (5×10^6) derived from BALB/c mice were also injected into the peritoneum of $PI3K^{-/-}$ mice to reconstitute peritoneal mast cells.

Culture of BMMCs in T_H2 conditions and CFSE labeling. $PI3K^{+/+}$ BMMCs were cultured for 3 days in CM supplemented with IL-4 (10 ng/ml) and IL-10 (10 ng/ml) to generate T_H2-conditioned BMMCs. T_H2-conditioned and nontreated BMMCs were resuspended in PBS and labeled with 10 μM 5(and 6)-carboxyfluorescein diacetate succinimidyl ester (CFSE, Molecular Probes, Eugene, OR) for 10 min at 37 °C. Cells were washed twice in PBS and resuspended in fresh ice-cold PBS.

Infection with *S. venezuelensis*. *S. venezuelensis*, a gift of Y. Nawa (Miyazaki Medical College), was maintained by serial passage in male Wistar rats; infectious larvae (L3) were obtained by fecal culture. Mice were infected by subcutaneous inoculation with 2000 L3. In selected experiments, infected $PI3K^{-/-}$ mice were given a series of intravenous injections with T_H2-conditioned or nontreated BMMCs (3×10^6–5×10^6) on days 3, 5 and 7 after infection. The extent of infection of individual mice was monitored by counting the number of parasites' eggs excreted in feces (eggs per gram of feces). The number of adult worms recovered from the small intestine was counted on day 13 after infection. To examine mastocytosis, tissue mast cells in the gastrointestinal tracts were analyzed under the normal or fluorescence microscope[59] to detect injected BMMCs labeled with CFSE. Tissue slides were prepared from gastrointestinal tracts of infected mice 12 days after infection.

Immunoblotting. Cells were lysed in a lysis buffer solution that consisted of 20 mM Tris-HCl (pH 7.4), 250 mM NaCl, 20 mM β-glycerophosphate, 1 mM sodium orthovanadate, 5 mM *p*-nitrophenylphosphate, 2 mM dithiothreitol, 1% aprotinin, 1 mM PMSF, 10 μg/ml leupeptin, 10 μg/ml pepstatin A and 1% Triton X100. Post-nuclear supernatants were obtained by centrifugation at 10,000*g* for 30 min. Cell lysates were boiled for 3 min in Laemmli's sample buffer solution, fractionated on SDS-PAGE, transferred to PVDF membranes and blotted with various antibodies. The reactive bands were visualized with horseradish peroxidase conjugated to the appropriate secondary antibodies with an enhanced chemiluminescence immunoblotting detection system (Amersham, Little Chalfont, UK).

Protein kinase assays. For p38 kinase analysis, active p38 immunoprecipitated with a monoclonal mouse anti–phospho-p38 (dually phosphorylated at Thr^{180} and Tyr^{182}, Cell Signaling Technology) was used to phosphorylate GST–ATF-2 (Cell Signaling Technology) for 30 min at 30 °C. The degree of ATF-2 phosphorylation, as p38 kinase activity, was determined by immunoblotting with anti-phospho–ATF-2 (Cell Signaling Technology). As standards, amounts of p38 were detected in whole-cell lysates with anti-p38α. For Jnk analysis, samples were incubated with GST–c-Jun and glutathione sepharose (Amersham) overnight to precipitate active Jnk. Kinase analysis was done with the addition of ATP to the complexes, followed by the kinase reaction for 30 min at 30 °C. Phospho–c-Jun was detected with anti-phospho–c-Jun (Cell Signaling Technology).

Detection of cytokines. Titers of mouse IL-3, IL-4, IL-5 and TNF-α were determined with specific Quantikine M ELISA kits from R&D Systems (R&D System, Minneapolis, MN).

Statistical analysis. Two-group comparisons were done with Student's *t*-tests. Intergroup differences were considered significant at $P<0.05$.

Acknowledgments

We thank M. Motouchi and K. Furuichi for animal care; S. Matsuda for valuable discussions; L. K. Clayton and J. Fujimoto for critical reading of the manuscript; and the Department of Dermatology of Keio University School of Medicine for experimental equipment. Supported by a Keio University Special Grant-in-Aid for Innovative Collaborative Research Project; a grant for the Research For The Future Program (JSPS-RFTF-97L00701) from the Japan Society for the Promotion of Science; a Grant-in-Aid for Scientific Research on Priority Areas (C) (13226112); a National Grant-in-Aid for the Establishment of a High-Tech Research Center in a Private University; a grant for the Promotion of the Advancement of Education and Research in Graduate Schools; and a Scientific Frontier Research Grant from the Ministry of Education, Culture, Sports, Science and Technology, Japan.

Competing interests statement

The authors declare that they have no competing financial interests.

Received 13 February 2001; accepted 29 January 2002.

1. Metcalfe, D. D., Baram, D. & Mekori, Y. A. Mast cells. *Physiol. Rev.* **77**, 1033–1079 (1997).
2. Galli, S. J. Mast cells and basophils. *Curr. Opin. Hematol.* **7**, 32–39 (2000).
3. Galli, S. J. & Hammel, I. Mast cell and basophil development. *Curr. Opin. Hematol.* **1**, 33–39 (1994).
4. Echtenacher, B., Mannel, D. N. & Hultner, L. Critical protective role of mast cells in a model of acute septic peritonitis. *Nature* **381**, 75–77 (1996).
5. Malaviya, R., Ikeda, T., Ross, E. & Abraham, S. N. Mast cell modulation of neutrophil influx and bacterial clearance at sites of infection through TNF-α. *Nature* **381**, 77–80 (1996).
6. Gurish, M. F. & Austen, K. F. The diverse roles of mast cells. *J. Exp. Med.* **194**, F1–5 (2001).
7. Shelburne, C. P. & Ryan, J. J. The role of Th2 cytokines in mast cell homeostasis. *Immunol. Rev.* **179**, 82–93 (2001).
8. Lantz, C. S. & Huff, T. F. Differential responsiveness of purified mouse c-kit$^+$ mast cells and their progenitors to IL-3 and stem cell factor. *J. Immunol.* **155**, 4024–4029 (1995).
9. Rodewald, H. R., Dessing, M., Dvorak, A. M. & Galli, S. J. Identification of a committed precursor for the mast cell lineage. *Science* **271**, 818–822 (1996).
10. Galli, S. J., Zsebo, K. M. & Geissler, E. N. The kit ligand, stem cell factor. *Adv. Immunol.* **55**, 1–96 (1994).
11. Kitamura, Y., Go, S. & Hatanaka, K. Decrease of mast cells in W/W^v mice and their increase by bone marrow transplantation. *Blood* **52**, 447–452 (1978).
12. Galli, S. J. & Kitamura, Y. Animal models of human disease. Genetically mast-cell-deficient W/W^v and Sl/Sl^d mice: their value for the analysis of the roles of mast cells in biological responses *in vivo*. *Am. J. Pathol.* **127**, 191–198 (1987).
13. Finkelman, F. D. *et al.* Cytokine regulation of host defense against parasitic gastrointestinal nematodes: Lessons from studies with rodent models. *Annu. Rev. Immunol.* **15**, 505–533 (1997).
14. Nawa, Y. *et al.* Selective effector mechanisms for the expulsion of intestinal helminths. *Parasite Immunol.* **16**, 333–338 (1994).
15. Reynolds, D. S. *et al.* Different mouse mast cell populations express various combinations of at least six distinct mast cell serine proteases. *Proc. Natl Acad. Sci. USA* **87**, 3230–3234 (1990).
16. Thompson-Snipes, L. *et al.* Interleukin 10: a novel stimulatory factor for mast cells and their progenitors. *J. Exp. Med.* **173**, 507–510 (1991).
17. Else, K. J., Finkelman, F. D., Maliszewski, C. R. & Grencis, R. K. Cytokine-mediated regulation of chronic intestinal helminth infection. *J. Exp. Med.* **179**, 347–351 (1994).
18. Kobayashi, T. *et al.* Intestinal mast cell response and mucosal defence against *Strongyloides venezuelensis* in interleukin-3-hyporesponsive mice. *Parasite Immunol.* **20**, 279–284 (1998).
19. Abe, T. & Nawa, Y. Kinetic study of mast-cell growth factor production by lymphocytes during the course of *Strongyloides ratti* infection in mice. *Parasitol. Res.* **74**, 484–488 (1988).
20. Urban, J. F. Jr *et al.* IL-13, IL-4Rα, and Stat6 are required for the expulsion of the gastrointestinal nematode parasite *Nippostrongylus brasiliensis*. *Immunity* **8**, 255–264 (1998).
21. Khan, W. I. *et al.* Critical role for signal transducer and activator of transcription factor 6 in mediating intestinal muscle hypercontractility and worm expulsion in *Trichinella spiralis*-infected mice. *Infect. Immunity* **69**, 838–844 (2001).
22. Carpenter, C. L. & Cantley, L. C. Phosphoinositide kinases. *Curr. Opin. Cell Biol.* **8**, 153–158 (1996).
23. Kinet, J. P. The high-affinity IgE receptor (FcεRI): from physiology to pathology. *Annu. Rev. Immunol.* **17**, 931–972 (1999).
24. Timokhina, I., Kissel, H., Stella, G. & Besmer, P. Kit signaling through PI 3-kinase and Src kinase pathways: an essential role for Rac1 and JNK activation in mast cell proliferation. *EMBO J.* **17**, 6250–6262 (1998).
25. Escobedo, J. A. *et al.* cDNA cloning of a novel 85 kd protein that has SH2 domains and regulates

binding of PI3-kinase to the PDGFβ-receptor. *Cell* **65**, 75–82 (1991).
26. Skolnik, E.Y. *et al.* Cloning of PI3 kinase-associated p85 utilizing a novel method for expression/cloning of target proteins for receptor tyrosine kinases. *Cell* **65**, 83–90 (1991).
27. Otsu, M. *et al.* Characterization of two 85 kd proteins that associate with receptor tyrosine kinases, middle-T/pp60$^{c\text{-}src}$ complexes, and PI3-kinase. *Cell* **65**, 91–104 (1991).
28. Terauchi, Y. *et al.* Increased insulin sensitivity and hypoglycemia in mice lacking the p85α subunit of phosphoinositide 3-kinase. *Nature Genet.* **21**, 230–235 (1999).
29. Suzuki, H. *et al. Xid*-like immunodeficiency in mice with disruption of the p85α subunit of phosphoinositide 3-kinase. *Science* **283**, 390–392 (1999).
30. Bochner, B. S. & Lichtenstein, L. M. Anaphylaxis. *N. Engl. J. Med.* **324**, 1785–1790 (1991).
31. Humphries, D. E. *et al.* Heparin is essential for the storage of specific granule proteases in mast cells. *Nature* **400**, 769–772 (1999).
32. Forsberg, E. *et al.* Abnormal mast cells in mice deficient in a heparin-synthesizing enzyme. *Nature* **400**, 773–776 (1999).
33. Dombrowicz, D., Flamand, V., Brigman, K. K., Koller, B. H. & Kinet, J. P. Abolition of anaphylaxis by targeted disruption of the high affinity immunoglobulin E receptor α chain gene. *Cell* **75**, 969–976 (1993).
34. Jacoby, W. P., Cammarata, V., Findlay, S. & Pincus, S. Anaphylaxis in mast cell-deficient mice. *J. Invest. Dermatol.* **83**, 302–304 (1984).
35. Takeishi, T., Martin, T. R., Katona, I. M., Finkelman, F. D. & Galli, S. J. Differences in the expression of the cardiopulmonary alterations associated with anti-immunoglobulin E-induced or active anaphylaxis in mast cell-deficient and normal mice. Mast cells are not required for the cardiopulmonary changes associated with certain fatal anaphylactic responses. *J. Clin. Invest.* **88**, 598–608 (1991).
36. Martin, T. R., Galli, S. J., Katona, I. M. & Drazen, J. M. Role of mast cells in anaphylaxis. Evidence for the importance of mast cells in the cardiopulmonary alterations and death induced by anti-IgE in mice. *J. Clin. Invest.* **83**, 1375–1383 (1989).
37. Lu-Kuo, J. M., Fruman, D. A., Joyal, D. M., Cantley, L. C. & Katz, H. R. Impaired kit- but not FcεRI-initiated mast cell activation in the absence of phosphoinositide 3-kinase p85α gene products. *J. Biol. Chem.* **275**, 6022–6029 (2000).
38. Nakano, T. *et al.* Fate of bone marrow-derived cultured mast cells after intracutaneous, intraperitoneal, and intravenous transfer into genetically mast cell-deficient W/W^{v} mice: evidence that cultured mast cells can give rise to both connective tissue type and mucosal mast cells. *J. Exp. Med.* **162**, 1025–1043 (1985).
39. Mekori, Y. A., Oh, C. K. & Metcalfe, D. D. IL-3-dependent murine mast cells undergo apoptosis on removal of IL-3. Prevention of apoptosis by c-kit ligand. *J. Immunol.* **151**, 3775–3784 (1993).
40. Tsai, M. *et al.* Induction of mast cell proliferation, maturation, and heparin synthesis by the rat c-kit ligand, stem cell factor. *Proc. Natl Acad. Sci. USA* **88**, 6382–6386 (1991).
41. Okuda, K. *et al.* Granulocyte-macrophage colony-stimulating factor, interleukin-3, and steel factor induce rapid tyrosine phosphorylation of p42 and p44 MAP kinase. *Blood* **79**, 2880–2887 (1992).
42. Foltz, I. N., Lee, J. C., Young, P. R. & Schrader, J. W. Hemopoietic growth factors with the exception of interleukin-4 activate the p38 mitogen-activated protein kinase pathway. *J. Biol. Chem.* **272**, 3296–3301 (1997).
43. Garrington, T. P. *et al.* MEKK2 gene disruption causes loss of cytokine production in response to IgE and c-Kit ligand stimulation of ES cell-derived mast cells. *EMBO J.* **19**, 5387–5395 (2000).
44. Datta, S. R., Brunet, A. & Greenberg, M. E. Cellular survival: a play in three Akts. *Genes Dev.* **13**, 2905–2927 (1999).
45. Lantz, C. S. *et al.* Role for interleukin-3 in mast-cell and basophil development and in immunity to parasites. *Nature* **392**, 90–93 (1998).
46. Friend, D. S. *et al.* Mast cells that reside at different locations in the jejunum of mice infected with *Trichinella spiralis* exhibit sequential changes in their granule ultrastructure and chymase phenotype. *J. Cell Biol.* **135**, 279–290 (1996).
47. Knight, P. A., Wright, S. H., Lawrence, C. E., Paterson, Y. Y. W. & Miller, H. R. P. Delayed expulsion of the nematode *Trichinella spiralis* in mice lacking the mucosal mast cell-specific granule chymase, mouse mast cell protease-1. *J. Exp. Med.* **192**, 1849–1856 (2000).
48. Khan, A. I., Horii, Y., Tiuria, R., Sato, Y. & Nawa, Y. Mucosal mast cells and the expulsive mechanisms of mice against *Strongyloides venezuelensis*. *Int. J. Parasitol.* **23**, 551–555 (1993).
49. Sato, Y. & Toma, H. Effects of spleen cells and serum on transfer of immunity to *Strongyloides venezuelensis* infection in hypothymic (nude) mice. *Int. J. Parasitol.* **20**, 63–67 (1990).
50. Ghildyal, N., McNeil, H. P., Gurish, M. F., Austen, K. F. & Stevens, R. L. Transcriptional regulation of the mucosal mast cell-specific protease gene, MMCP-2, by interleukin 10 and interleukin 3. *J. Biol. Chem.* **267**, 8473–8477 (1992).
51. Ghildyal, N. *et al.* IL-10 induces transcription of the gene for mouse mast cell protease-1, a serine protease preferentially expressed in mucosal mast cells of *Trichinella spiralis*-infected mice. *J. Immunol.* **149**, 2123–2129 (1992).
52. Ghildyal, N., Friend, D. S., Nicodemus, C. F., Austen, K. F. & Stevens, R. L. Reversible expression of mouse mast cell protease 2 mRNA and protein in cultured mast cells exposed to IL-10. *J. Immunol.* **151**, 3206–3214 (1993).
53. Abe, T. & Nawa, Y. Reconstitution of mucosal mast cells in W/W^{v} mice by adoptive transfer of bone marrow-derived cultured mast cells and its effects on the protective capacity to *Strongyloides ratti*-infection. *Parasite Immunol.* **9**, 31–38 (1987).
54. Kissel, H. *et al.* Point mutation in kit receptor tyrosine kinase reveals essential roles for kit signaling in spermatogenesis and oogenesis without affecting other kit responses. *EMBO J.* **19**, 1312–1326 (2000).
55. Suzuki, K. *et al.* Role of common cytokine receptor γ chain (γ_c)- and Jak3-dependent signaling in the proliferation and survival of murine mast cells. *Blood* **96**, 2172–2180 (2000).
56. Godfraind, C. *et al.* Intraepithelial infiltration by mast cells with both connective tissue-type and mucosal-type characteristics in gut, trachea, and kidneys of IL-9 transgenic mice. *J. Immunol.* **160**, 3989–3996 (1998).
57. Finkelman, F. D. *et al.* Effects of interleukin 12 on immune responses and host protection in mice infected with intestinal nematode parasites. *J. Exp. Med.* **179**, 1563–1572 (1994).
58. Yamaguchi, M. *et al.* IgE enhances mouse mast cell FcεRI expression *in vitro* and *in vivo*: Evidence for a novel amplification mechanism in IgE-dependent reactions. *J. Exp. Med.* **185**, 663–672 (1997).
59. Fukao, T. *et al.* Inducible expression of Stat4 in dendritic cells and macrophages and its critical role in innate and adaptive immune responses. *J. Immunol.* **166**, 4446–4455 (2001).

Hum Genet (2003) 112 : 244–248
DOI 10.1007/s00439-002-0870-8

ORIGINAL INVESTIGATION

**Vahid Khajoee · Kenji Ihara · Ryutaro Kira
Megumi Takemoto · Hiroyuki Torisu · Yasunari Sakai
Jia Guanjun · Park Myoung Hee · Katsushi Tokunaga
Toshiro Hara**

Founder effect of the *C9* R95X mutation in Orientals

Received: 9 August 2002 / Accepted: 22 October 2002 / Published online: 9 January 2003

Abstract A nonsense mutation at codon 95 (R95X) in the *C9* gene is responsible for most Japanese C9 deficiency (C9D) cases, with a carrier frequency of 6.7%. Upon analysis of microsatellite markers and newly identified dinucleotide repeat number polymorphisms in the 3′ flanking region of the *C9* gene, a founder effect was demonstrated for the R95X mutation of the *C9* gene in Japanese. Screening for the R95X mutation in Korean and Chinese individuals showed that the R95X carrier frequencies in Koreans and Chinese were 2.0% and 1.0%, respectively. Although homozygotes for the R95X mutation were not found in Korea or China, the shared haplotype of the dinucleotide repeat number polymorphisms appeared to be associated with the R95X mutation in the heterozygotes in Korea and China. The founder effect found in East Asians (Japanese, Koreans and Chinese) but not in Caucasians, as well as the haplotype sharing in only a small chromosomal interval, suggested that the R95X mutation of *C9* gene was ancient and had occurred after the divergence of East Asians and Caucasians, and before migration of the Yayoi people to Japan. Since the mortality of meningococcal infections in complement-deficient patients is lower than that in normal individuals, a founder effect and a selective advantage in isolation might be the main reasons for the high frequency of the R95X mutation in Japan.

V. Khajoee · K. Ihara · R. Kira (✉) · M. Takemoto · H. Torisu
Y. Sakai · T. Hara
Department of Pediatrics, Graduate School of Medical Sciences,
Kyushu University,
3-1-1 Maidashi, 812-8582 Higashi-Ku, Fukuoka, Japan
Tel.: +81-92-6425421, Fax: +81-92-6425435,
e-mail: kirari@pediatr.med.kyushu-u.ac.jp

J. Guanjun
Harbin Red Cross Blood Center, Harbin, China

P. M. Hee
Department of Clinical Pathology,
Seoul National University College of Medicine,
Seoul, South Korea

K. Tokunaga
Department of Human Genetics,
Graduate School of International Health, University of Tokyo,
Tokyo, Japan

Introduction

Complement component 9 (*C9*) is one of the constituents of the membrane attack complex (MAC), which causes lysis and death of target cells upon activation of the complement system (O'Hara et al. 2001). *C9* deficiency (C9D) (MIM: 120940) is inherited as an autosomal recessive trait (Winkelstein et al. 1995), and is one of the most frequent genetic disorders in Japan, with an incidence of about 1/1,000 (Fukumori et al. 1989; Hayama et al. 1989), but is very rare in Caucasians (Zoppi et al. 1990; Wurzner et al. 1992). Although most C9D individuals are healthy, C9D individuals have a much higher risk for developing meningococcal meningitis than normal controls (Nagata et al. 1989).

A nonsense mutation at codon 95 (R95X) in exon 4 of the *C9* gene is responsible for most Japanese C9D cases, as indicated by two independent studies (Kira et al. 1998; Horiuchi et al. 1998). Indeed, one in 15 (6.7%) of normal individuals was found to have the R95X mutation in Japan; the estimated frequency of C9D individuals being around 0.12%, which is consistent with the frequency revealed by serological studies (Fukumori et al. 1989; Hayama et al. 1989).

Studies on the molecular basis of C9D in European and Japanese populations (Horiuchi et al. 1998; Kira et al. 1998; Witzel-Schlomp et al. 1997, 1998) revealed a great difference in the mutation sites between the two populations. A very high prevalence of the R95X mutation only in Japanese has prompted us to investigate (1) whether the high frequency of the R95X mutation in Japanese is the result of a founder effect or a mutational hot spot, (2) whether this R95X mutation is observed in other Asian countries near Japan, and (3) whether it has a common ancestral origin in East Asia.

With three microsatellite markers near the *C9* gene, and newly identified $(CA)_n$ and $(GT)_n$ repeat number polymor-

Table 1 Genotypic analysis of Japanese C9D patients

Markers	C9D patients genotypes					Major alleles in normal Japanese (%)
	1	2	3	4	5	
D5S2082	1/1	1/1	2/2	2/2	2/3	2 (71.0), 1 (26.0)
D5S634	3/3	3/3	3/3	4/4	3/4	3 (58.3), 4 (31.0)
R95X mutation	+/+	+/+	+/+	+/+	+/+	-/-
$(CA)_n$	12/12	12/12	12/12	12/12	12/12	Table 3
$(GT)_n$	20/20	20/20	20/20	20/20	20/20	Table 4
D5S1994	4/5	4/7	4/5	4/4	4/4	4 (37.6), 5 (25.0)

phisms in the 3′ flanking region of the *C9* gene, we have first demonstrated that the high frequency of the R95X mutation in Japanese is the result of a founder effect, and then that the R95X mutation was present in other Asian countries as well. Through haplotype analysis of the R95X mutation and adjacent markers in Japan, Korea and China, the present study has revealed the presence of a common founder mutation in these countries.

Subjects and methods

Study subjects

The study populations were from three countries, Japan, Korea and China. The Japanese genomic DNA samples were from 100 normal children, 18 heterozygotes for the R95X mutation and five C9D patients (homozygotes), whose genotypes were determined in our previous studies (Kira et al. 1998, 1999). Genomic DNA samples were also obtained from 200 individuals in Seoul city in South Korea and 195 in Harbin city in the northeast of China. The diagnosis of selective complete C9D was made by functional and genetic analyses (Nagata et al. 1989; Kira et al. 1999). Informed consent was obtained from the parents of all cases before study. The Ethics Committee of Kyushu University approved this study.

DNA extraction

Genomic DNA was isolated from peripheral blood leukocytes using the extraction kit, QIAamp Blood Kit (QIAGEN, Tokyo, Japan).

Allele-specific PCR

Allele-specific PCR for exon 4 of the *C9* gene was performed to detect the R95X mutation as previously described (Kira et al. 1998), with the same PCR profile. The common and normal primers (N primer set) were used for the normal *C9* gene, and the common and mutant primers (M primer set) for the R95X mutant gene. The DNA samples were amplified with each primer set and the PCR products were visualized in a 1.5% agarose gel by ethidium bromide staining. To confirm R95X heterozygous individuals, SSCP analysis was performed as described previously (Kira et al. 1999).

Marker analysis

Genotyping of markers was performed in 40 normal individuals in each country, and all heterozygotes and homozygotes for the R95X mutation. The *C9* 3′ flanking region, containing the $(CA)_n$ and $(GT)_n$ repeat, was amplified with the following primer pairs: $(CA)_n$ repeat, forward 5′-AAGTGCTATATACCCAAGAT-3′ and reverse 5′-GAAGACTGAAAAATTGACAC-3′; and $(GT)_n$ repeat, forward 5′-CCAGCCTCATTGTTTCTTA-3′ and reverse 5′-TGGCACACATGTACCTATG-3′. The 5′ ends of both forward primers were fluorescence-labeled with 6-carboxyfluorescein dye. PCR was carried out in a total volume of 25 µl containing 20 ng of genomic DNA, 10 pmol of each primer, 0.625 units of *Taq* DNA polymerase and 0.2 nmol of each deoxynucleoside triphosphate. The PCR profile was as follows: initial denaturation at 94 °C for 3 min, followed by 40 cycles of 94 °C for 30 s, 60 °C for 30 s, and 72 °C for 30 s, with final extension of 72 °C for 5 min. Genotyping was performed in a mixture of amplified products and an internal size standard by ABI PRISM 310 genetic analyzer (Applied Biosystems, Foster City, Calif., USA). Several representative samples were sequenced with ABI PRISM 3100 (Applied Biosystems) to confirm the authenticity of the GeneScan results.

PCR was performed for microsatellite markers D5S634 (Gyapay et al. 1994), D5S2082 and D5S1994 (Dib et al. 1996). Using fluorescent primers, genotyping was performed as described above.

Statistical analysis

Chi-squared analysis was performed using software package Statview version 4.5. The frequencies of the (CA)-(GT) haplotype in two repeat number polymorphisms were estimated using the Estimating Haplotype-frequencies (EH) software program (http://linkage.rockefeller.edu/ott/eh.htm). *P* values of less than 0.05 were considered to be significant.

Results

On analysis of microsatellite markers D5S2082, D5S634, and D5S1994 in five Japanese patients with C9D, no common alleles were observed, as shown in Table 1. As the microsatellite markers were far from the *C9* gene, as shown in Fig. 1, we then examined two sites of dinucleotide repeat number polymorphisms in the 3′ flanking

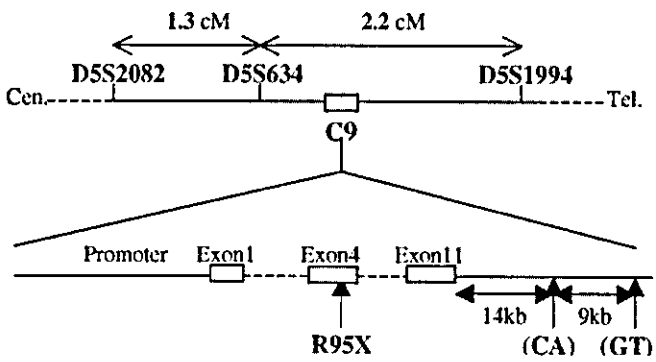

Fig. 1 Schematic genomic organization of microsatellite markers, and two repeat number polymorphisms adjacent to and within the *C9* gene

region of the *C9* gene. The $(CA)_{12}$ and $(GT)_{20}$ alleles were common in all the C9D patients, indicating the presence of a founder effect of the *C9* R95X mutation. Haplotype analysis in Japanese demonstrated that the $(CA)_{12}$-$(GT)_{20}$ haplotype was significantly associated with the R95X mutation in homozygotes, as well as in heterozygotes (P <0.0001) (Table 2).

Next, to determine whether the R95X mutation could be observed in Asian countries other than Japan, the R95X mutation was screened for in Korean and Chinese individuals. Four and two heterozygotes for the R95X mutation were found among 200 Korean and 195 Chinese individuals, respectively. The R95X carrier frequencies for Koreans and Chinese were thus 2.0% and 1.0%, respectively. Although there were no homozygotes among them, these data strongly suggested that C9D individuals do exist in Asian countries other than Japan.

Then, to determine whether a common founder existed in Japan and other Asian countries, the $(CA)_n$ and $(GT)_n$ polymorphisms were examined in Korean and Chinese individuals. Regarding the $(CA)_n$ repeat number polymorphism, $(CA)_{12}$ and $(CA)_{13}$ repeat alleles were identified in three wild-type populations and their R95X heterozygotes (Table 3). Consistent with the fact that all the Japanese homozygotes for the R95X mutation had only the $(CA)_{12}$ allele, all the heterozygotes in Japan, Korea and China carried at least one $(CA)_{12}$ allele. The $(CA)_n$ allele frequencies did not exhibit any significant differences among Korean, Chinese and Japanese wild-type individuals in the whole allele distribution or on the respective allele comparison. With respect to the $(GT)_n$ polymorphism, there were ten types of repeat number, ranging from 15 to 24, in three wild-type populations and R95X heterozygotes (Table 4). All the heterozygotes in Japan, Korea and China had

Table 2 Estimated haplotype frequencies in two-dinucleotide repeat number polymorphisms in Japanese individuals. The P value for each haplotype frequency was calculated by Chi-squared test with a 2×3 contingency table (*NS* not significant)

Haplotype	Haplotype frequency (%)			P value
	Wild type individuals	Heterozygotes for R95X mutation	Homozygotes for R95X mutation	
CA_{12}-GT_{20}	29.1	64.8	100.0	<0.0001
CA_{12}-GT_{21}	22.9	3.1	0.0	0.0075
CA_{12}-GT_{19}	13.5	12.5	0.0	NS
CA_{13}-GT_{20}	12.1	7.3	0.0	NS
CA_{12}-GT_{16}	6.2	5.5	0.0	NS
Minor haplotypes	16.2	6.8	0.0	NS

Table 3 Allele frequencies of *C9* gene $(CA)_n$ repeat number polymorphisms in heterozygotes for the R95X mutation and wild type subjects in Chinese, Korean and Japanese populations

Allele	Allele frequency					
	Chinese		Korean		Japanese	
	wild type	R95X heterozygotes	wild type	R95X heterozygotes	wild type	R95X heterozygotes
	n=80 (%)	n=4 (%)	n=80 (%)	n=8 (%)	n=80 (%)	n=36 (%)
$(CA)_{12}$	59 (73.7)	2 (50.0)	61 (76.3)	8 (100)	60 (75.0)	32 (88.9)
$(CA)_{13}$	21 (26.3)	2 (50.0)	19 (23.7)	0 (0.0)	20 (25.0)	4 (11.1)

Table 4 Allele frequencies of *C9* gene $(GT)_n$ repeat number polymorphisms in heterozygotes for the R95X mutation and wild-type subjects in Chinese, Korean and Japanese populations. The differences in respective allele frequencies between the wild-type and R95X heterozygote groups in each country, and those between the wild-type or R95X heterozygote groups in two countries were evaluated using the χ^2 test for 2×2 tables; P values <0.05 are indicated

Allele	Allele frequency					
	Chinese		Korean		Japanese	
	wild type	R95X hetrozygotes	wild type	R95X hetrozygotes	wild type	R95X hetrozygotes
	n=80 (%)	n=4 (%)	n=80 (%)	n=8 (%)	n=80 (%)	n=36 (%)
$(GT)_{15-18}$	10 (12.5)	0 (0.0)	12 (15.0)	0 (0.0)	11 (13.8)	2 (5.6)
$(GT)_{19}$	15 (18.7)	2 (50.0)	18 (22.5)	0 (0.0)	14 (17.5)	5 (13.8)
$(GT)_{20}$	45 (56.3)	2 (50.0)	40 (50.0)	7 (87.0)	33 (41.2) [a]	26 (72.2) [a]
$(GT)_{21}$	6 (7.5) [c]	0 (0.0)	7 (8.7) [d]	0 (0.0)	20 (25.0) [b,c,d]	2 (5.6) [b]
$(GT)_{22-24}$	4 (5.0)	0 (0.0)	3 (3.7)	1 (13.0)	2 (2.5)	1 (2.8)

[a]Japanese; wild-type vs R95X heterozygotes, P =0.0025
[b]Japanese; wild type vs R95X heterozygotes, P =0.0193
[c]Wild type; Japanese vs Chinese, P =0.0046
[d]Wild type; Japanese vs Korean, P =0.0103

at least one $(GT)_{20}$ repeat allele, compatible with the finding that the $(GT)_{20}$repeat allele was observed in Japanese homozygotes for the R95X mutation. The $(GT)_n$ allele frequencies did not exhibit any significant differences between Korean and Chinese wild-type individuals in the whole allele distribution or on the respective allele comparison; however, Japanese wild-type individuals exhibited a significantly higher $(GT)_{21}$ allele frequency than Korean and Chinese controls (P value=0.0103 and 0.0046, respectively). Although homozygotes for the R95X mutation were not found in Korea or China, the $(CA)_{12}$-$(GT)_{20}$ haplotype appeared to be associated with the R95X mutation in heterozygotes. The genotype distributions in Chinese, Korean and Japanese control groups were under the Hardy-Weinburg equilibrium (data not shown).

Discussion

The R95X mutation in exon 4 of the *C9* gene is the predominant mutation in C9D individuals in Japan, the carrier frequency being around 6.7%. This study is the first to demonstrate that the R95X mutation occurs in normal Chinese and Korean individuals, with carrier frequencies of 1.0% and 2.0%, while the frequencies of C9D in Chinese and Korean individuals were estimated to be 1/40,000 and 1/10,000, respectively. On haplotype analysis, we found that the high frequency of the R95X mutation results from a founder effect rather than a mutational hot spot in Japanese, and in Koreans and Chinese as well.

Fig 2 Location of four cities in Japan, Korea and China, with the frequencies of the R95X mutation

Thus, the frequency of the R95X mutation with a common ancestral origin showed a gradual increase in geographic order from China, the Korean peninsula and then to the Japan Archipelago (Fig. 2).

There are many theories and much controversy regarding the origins of the Japanese population based on studies by anthropologists, archaeologists and geneticists (Omoto and Saitou 1997). Hondo (main islands)-Japanese are thought to be mainly derived from the migrants from the north/northeast of the Asian continent around the Aeneolithic Yayoi period (300 B.C.–300 A.D.) (Tokunaga et al. 1996; Omoto and Saitou 1997; Normile 1999). Therefore, it is possible that the R95X mutation, with a widespread geographic distribution, was derived from a founder mutation, which spread throughout north/northeast Asia and finally to Japan as a result of migration.

There are a number of diseases, such as Fukuyama-type congenital muscular dystrophy, with a founder effect found only in Japan (i.e., not in Korea or China), suggesting that such mutations originated from the Yayoi people during or after migration to Japan (Toda et al. 1999). On the other hand, Wang et al. (1991) reported a founder effect of the phenylketonuria mutation in Chinese and Japanese. Similar to the phenylketonuria mutation, the R95X mutation of the *C9* gene appears to have occurred after the divergence of East Asians and Caucasians, and before migration of the Yayoi people to Japan. In addition, the R95X mutation is considered to be ancient because haplotype sharing has been observed in only a small chromosomal interval (Fig. 1).

The major proportion of the Japanese population is known to be relatively homogeneous, probably because Japan comprises isolated islands, and thus there has been less migration. Since there were differences in the allele frequencies between Korean and Japanese normal individuals, it is possible that the R95X mutation has been maintained at a high frequency in the Japanese population partly through a bottle-neck effect during migration from the Asian continent to Japan. In addition, in ancient times, C9D individuals might have had a selective advantage because the mortality from meningococcal infections in complement-deficient patients was lower than that in normal individuals, probably due to the attenuated inflammatory response in the absence of MAC (Ross and Densen 1984; Lehner et al. 1992). Similarly, the C2 deficiency is the most common complement deficiency in Caucasians with a founder mutation, and its carrier frequency is relatively high (1.0–2.0%) (Johnson et al. 1992). Considering the lower mortality, a selective advantage might be another reason for the extreme predominance of C9D in Japanese, as well as for the C2 deficiency in Caucasians.

In conclusion, a founder effect and a selective advantage in isolation might be the main reasons for the high frequency of the R95X mutation in Japan.

Acknowledgements We would like to thank Drs. Chie Harashima and Saifuddin Ahmed for their technical assistance. This work was supported by a grant from the Ministry of Education, Culture, Sports, Science and Technology of Japan.

References

Dib C, Faure S, Fizames C, Samon D, Drouot N, Vignal A, Millasseau P, Marc S, Hazan J, Seboun E, Lathrop M, Gyapay G, Morissette J, Weissenbach J (1996) A comprehensive genetic map of the human genome based on 5,264 microsatellites. Nature 380:152–154

Fukumori Y, Yoshimura K, Ohnoki S, Yamaguchi H, Akagaki Y, Inai S (1989) A high incidence of C9 deficiency among healthy blood donors in Osaka, Japan. Int Immunol 1:85–89

Gyapay G, Morissette J, Vignal A, Dib C, Fizames C, Millasseau P, Mark S, Bernardi G, Lathrop M, Weissenbach J (1994) The 1993–94 Genethon human genetic linkage map. Nat Genet 7: 246–249

Hayama K, Sugai N, Tanaka S, Lee S, Kikuchi H, Ito J, Suzuki J, Nagata Y, Kondo H, Harayama O, et al. (1989) High-incidence of C9 deficiency throughout Japan: there are no significant differences in incidence among eight areas of Japan. Int Arch Allergy Appl Immunol 90:400–404

Horiuchi T, Nishizaka H, Kojima T, Sawabe T, Niho Y, Schneider PM, Inaba S, Sakai K, Hayashi K, Hashimura C, Fukumori Y (1998) A non-sense mutation at Arg95 is predominant in complement 9 deficiency in Japanese. J Immunol 160:1509–1513

Johnson CA, Densen P, Hurford RK, Colten HR, Wetsel RA (1992) Type I human complement C2 deficiency. A 28-base pair gene deletion causes skipping of exon 6 during RNA splicing. J Biol Chem 267:9347–9353

Kaufmann T, Hansch G, Rittner C, Spath P, Tedesco F, Schneider PM (1993) Genetic basis of human complement C8 beta deficiency. J Immunol 150:4943–4947

Kira R, Ihara K, Takada H, Gondo K, Hara T (1998) Nonsense mutation in exon 4 of human complement C9 gene is the major cause of Japanese complement C9 deficiency. Hum Genet 102: 605–610

Kira R, Ihara K, Watanabe K, Kanemitsu S, Ahmed SU, Gondo K, Takeshita K, Hara T (1999) Molecular epidemiology of C9 deficiency heterozygotes with an Arg95Stop mutation of the *C9*gene in Japan. J Hum Genet 44:109–111

Lehner PJ, Davies KA, Walport MJ, Cope AP, Würzner R, Orren A, Morgan BP, Cohen J (1992) Meningococcal septicaemia in a C6-deficient patient and effects of plasma transfusion on lipopolysaccharide release. Lancet 340: 1379–1381

Matsumoto H, Miyazaki T, Xu X, Watanabe H, Kawai N, Suzuki K (1986) Distribution of Gm and Km allotypes among five populations in China. Am J Phys Anthropol 70:161–165

Matsumoto H (1988) Characteristics of Mongoloid and neighbouring populations based on the genetic markers of human immunoglobulins. Hum Genet 80:207–218

Muller-Eberhard HJ (1986) The membrane attack complex of complement. Annu Rev Immunol 4:503–528

Nagata M, Hara T, Aoki T, Mizuno Y, Akeda H, Inaba S, Tsumoto K, Ueda K (1989) Inherited deficiency of ninth component of complement: an increased risk of meningococcal meningitis. J Pediatr 114:260–264

Normile D (1999) Genetic clues revise view of Japanese roots. Science 283:1426–1427

O'Hara AM, Moran AP, Würzner R, Orren A (2001) Complement-mediated lipopolysaccharide release and outer membrane damage in *Escherichia coli* J5: requirement for C9. Immunology 102: 365–372

Omoto K, Saitou N (1997) Genetic origins of the Japanese: a partial support for the dual structure hypothesis. Am J Phys Anthropol 102:437–446

Ross SC, Densen P (1984) Complement deficiency states and infection: epidemiology, pathogenesis and consequences of neisserial and other infections in an immune deficiency. Medicine (Baltimore) 63:243–273

Saucedo L, Ackermann L, Platonov AE, Gewurz A, Rakita RM, Densen P (1995) Delineation of additional genetic bases for C8 beta deficiency. Prevalence of null alleles and predominance of C→T transition in their genesis. J Immunol 155: 5022–5028

Toda T, Kobayashi K, Konda-Iida E, Sasaki J, Nakamura Y (1999) The Fukuyama congenital muscular dystrophy story. Neuromuscul Disord 10:153–159

Tokunaga K, Imanishi T, Takahashi K, Juji T (1996) On the origin and dispersal of East Asian populations as viewed from HLA haplotype. In: Akazawa T, Szathmary EJE (eds) Prehistoric Mongoloid Dispersals. Oxford University Press, Oxford, pp 187–97

Wang T, Okano Y, Eisensmith RC, Harvey ML, Lo WH, Huang SZ, Zeng YT, Yuan LF, Furuyama JI, Oura T, et al. (1991) Founder effect of a prevalent phenylketonuria mutation in the Oriental population. Proc Natl Acad Sci USA 88:2146–2150

Winkelstein JA, Sullivan KE, Colten HR (1995) Genetically determined disorders of the complement system. In: Scriver CR, Beaudet AL, Sly WS, Valle D (eds) The metabolic and molecular bases of inherited disease. 7th edn. McGraw-Hill, New York, pp 3911–3943

Witzel-Schlömp K, Spath PJ, Hobart MJ, Fernie BA, Rittner C, Kaufmann T, Schneider PM (1997) The human complement C9 gene: identification of two mutations causing deficiency and revision of the gene structure. J Immunol 158:5043–5049

Witzel-Schlömp K, Hobart MJ, Fernie BA, Orren A, Würzner R, Rittner C, Kaufmann T, Schneider PM (1998) Heterogeneity in the genetic basis of human complement C9 deficiency. Immunogenetics 48:144–147

Witzel-Schlömp K, Rittner C, Schneider PM (2001) The human complement C9 gene: structural analysis of the 5′ gene region and genetic polymorphism studies. Eur J Immunogenet 28:515–522

Würzner R, Orren A, Lachmann PJ (1992) Inherited deficiencies of the terminal components of human complement. Immunodefic Rev 3:123–147

Zoppi M, Weiss M, Nydegger UE, Hess T, Späth PJ (1990) Recurrent meningitis in a patient with congenital deficiency of the C9 component of complement. First case of C9 deficiency in Europe. Arch Intern Med 150:2395–2399

Hum Genet (2003) 112 : 348–352
DOI 10.1007/s00439-002-0897-x

ORIGINAL INVESTIGATION

Norimoto Kobayashi · Kazunaga Agematsu
Kanji Sugita · Masahiro Sako · Shigeaki Nonoyama
Akihiro Yachie · Satoru Kumaki · Shigeru Tsuchiya
Hans D. Ochs · Katsuo Sugita · Yoshimitsu Fukushima
Atsushi Komiyama

Novel *Artemis* gene mutations of radiosensitive severe combined immunodeficiency in Japanese families

Received: 17 September 2002 / Accepted: 27 November 2002 / Published online: 19 February 2003

Abstract A subgroup of patients with severe combined immunodeficiency (SCID) and increased cellular radiation sensitivity (RS-SCID) have mutations of *Artemis*, a gene that encodes a protein essential for V(D)J recombination and DNA double-strand break repair. RS-SCID described to date are either of European origin or are Athabascan-speaking native Americans belonging to the Navajo and Apache tribes. We have identified three Japanese boys and one girl from four unrelated families with RS-SCID caused by a genomic exon 3 deletion of the *Artemis* gene, resulting in loss of exon 3 and skipping of exon 4. Two patients were homozygous and two patients were heterozygous for this novel mutation. Those parents studied were heterozygous for this mutation. These findings suggest the genomic exon 3 deletion is unique to Japan and may be considered as a founder haplotype. Although two infants underwent successful bone marrow transplantation and immune reconstitution, the long-term outcome of this procedure is uncertain, because *Artemis* is expressed in most tissues and lack of its function in cells other than those derived from hematopoietic stem cells may increase the risk of malignancies.

N. Kobayashi · K. Agematsu (✉) · A. Komiyama
Department of Pediatrics,
Shinshu University School of Medicine,
Asahi 3-1-1, 390–8621 Matsumoto, Japan
Tel.: +81-263-372642, Fax: +81-263-373089,
e-mail: agemats@gipac.shinshu-u.ac.jp

K. Sugita
Department of Pediatrics, Yamanashi Medical University,
Yamanashi, Japan

M. Sako
Department of Pediatrics, Osaka City General Hospital,
Osaka, Japan

S. Nonoyama
Department of Pediatrics, Tokyo Medical and Dental University,
Tokyo, Japan

A. Yachie
Department of Laboratory Science, School of Health Sciences,
Faculty of Medicine, Kanazawa University, Kanazawa, Japan

S. Kumaki · S. Tsuchiya
Department of Immunology,
Tohoku University School of Medicine, Sendai, Japan

H. D. Ochs
Department of Pediatrics,
University of Washington School of Medicine, Seattle, USA

K. Sugita
Department of Biochemistry, Faculty of Medicine,
Chiba University, Chiba, Japan

Y. Fukushima
Department of Hygiene and Medical Genetics,
Shinshu University School of Medicine, Matsumoto, Japan

Introduction

Severe combined immunodeficiency (SCID) is a rare genetic disorder characterized by profoundly defective T lymphocytes and serum antibodies. In one form of SCID, both circulating T and B lymphocytes are absent because of a defect in the V(D)J recombination process, whereas natural killer (NK) cells are normally present (T^-B^- SCID). Mutations in either of the recombinase activating genes (*RAG1* or *RAG2* account for most of the patients with T^-B^- SCID (Schwarz et al. 1996; Corneo et al. 2000; Villa et al. 2001). However, in a subset of T^-B^- SCID, the defect is not caused by *RAG1* or *RAG2* mutations and is accompanied by a characteristic sensitivity to ionizing radiations (Cavazzana-Calvo et al. 1993).

In recent reports, Mochous et al. (2000, 2001) have demonstrated that T^-B^- SCID with increased cellular radiosensitivity (RS-SCID) is caused by mutations of *Artemis*, a gene that encodes for a key protein essential for V(D)J recombination and DNA double-strand breaks. Artemis, expressed in a broad range of broad tissues, forms a complex with DNA-dependent protein kinase (DNA-PK). Following complex formation, Artemis is phosphorylated by DNA-PK, a prerequisite for its endonuclease activity on 5' and 3' overhangs, and on hairpins, which are generated by the RAG complex. Thus, the Artemis/DNA-PK complex is essential for the hairpin-opening step of V(D)J

recombination and for 5' and 3' overhang processing in nonhomologous DNA end joining (Ma et al. 2002). To date, 13 predominantly RS-SCID patients with a variety of *Artemis* gene mutations and a large group of Athabascan-speaking native Americans from the Navajo and Apache tribes with a nonsense mutation of *Artemis* have been identified (Moshous et al. 2001; Li et al. 2002). We report here four Japanese RS-SCID patients with two novel mutations of the *Artemis* gene. Our results suggest that at least one of these mutations, the genomic deletion of exon 3, is a common mutation for Japanese T^-B^- SCID.

Materials and methods

Patients

Four Japanese patients were identified as SCID and as having coding regions of both *RAG1* and *RAG2* genes of the wild type. Patient 2 was the offspring of second-cousin parents, and the other three children were born to non-consanguineous patients. Each of the four patients was born full term after a normal pregnancy and appeared well until their first infection at 2–4 months of age (Table 1). Severe hypogammmaglobulinemia was a consistent finding. In these patients, both T and B lymphocytes were absent in the peripheral blood, but NK cells were present in a normal quantity. Patient 2 lacked B cells but had $CD3^+$ T cells (25%) that were, however, $CD4^+$ cells. In situ hybridization analysis to identify the X/Y chromosomes revealed that all the $CD3^+$ lymphocytes sorted in patient 2 were of female karyotype, implying the engraftment of maternal $CD4^+$ T cells in this male patient. In all infants, adenosine deaminase activity was normal. Patients 1 and 2 had successful hematopoietic stem-cell transplantation with or without conditioning and are completely immune-reconstituted. Patients 3 and 4 died of severe cytomegalovirus infection and of bronchiolitis obliterans after bone marrow transplantation, respectively.

Cells

Informed consent was obtained from the families and healthy controls prior to this study. Skin fibroblast cell lines from the patients were obtained from skin biopsies and cultured in RPMI1640 with 20% fetal calf serum (FCS).

Analysis of sensitivity to irradiation

Primary fibroblasts were obtained from the patients and maintained in complete culture medium consisting of RPMI1640 supplemented with 15% FCS. The surviving fraction was determined after increasing doses (0.5–6 Gy) of γ-irradiation.

Mutation analysis of the *Artemis* gene

DNA and RNA were extracted from patient fibroblasts and from peripheral blood samples of the family members and normal controls. The *Artemis* gene is composed of 14 exons. Total RNA was amplified by the polymerase chain reaction (PCR) with the following primers containing exons 1–14: 5'-GGCGCTATGAGTTCTTTCGAG (sense); 5'-CTTAGGTATCTAAGAGTGAGC (anti-sense). Amplified RNA was subcloned by using the TA cloning kit (Takara, Tokyo, Japan) and sequenced.

To determinate the genomic exon 3 deletion, we used the nested PCR technique. A "long" PCR product was generated with primers of genomic DNA encompassing the deletion: 5'-GAAATGAAGTAAGAGTGGAGGGCTAGAAG (sence), located upstream of exon 2, and 5'-AGCAGCATTCTTCATACTAGCCAAAAGGTG (antisence), located downstream of exon 4, under stringent conditions, viz., 94°C for 1 min (1 cycle), 94°C for 20 s, 68°C for 20 min (14 cycles), 98°C for 20 s, 68°C for 20 min plus 15 s/cycle (16 cycles), 72°C for 10 min (1 cycle) by using Expand Long Template PCR (Takara). The second PCR (nested) was performed by amplifying the first reaction ("long" PCR) with the following pairs (1 pair each for exon 2, exon 3, and exon 4): E2F 5'-TTGGATGGCTCAGAAATGGGCAGC-3'; E2R 5'-GAGGGGTCTGGGATATTGGT-3'; E3F 5'-CAAGTAACAATGGTGAGGGAC-3'; E3R 5'-TGCCTCAGCCTCACAAGTAGC-3'; E4F 5'-CAGAGAGAGAGGGGAATGG-3'; E4R 5'-TGAGCATTCAAAATCA.

Results

The fibroblasts from patients showed a remarkably increased sensitivity towards X-rays, in comparison to primary fibroblasts obtained from normal individual (Fig. 1).

The reverse transcription/PCR (RT-PCR) products obtained from mRNA from Patients 1–3 and normal controls are shown in Fig. 2. The length of the predominant cDNA

Table 1 Clinical and laboratory data

Characteristic	Patient 1	Patient 2	Patient 3	Patient 4
Sex	Male	Male	Male	Female
Age at onset of symptoms	2 months	3 months	2 months	4 months
Types of Infections	Otitis/stomatitis	Otitis/diarrhea	Pneumonia (CMV)	Pneumonia/diarrhea
Immunoglobulins	(at time of diagnosis)			
IgG (mg/dl)	100	13	121	43
IgM (mg/dl)	3	2	<6	<0.9
IgA (mg/dl)	5	2	<5	<1.3
WBC (/mm^3)	5,700	17,570	11,090	3,160
Lymphocytes (%)	9	13	4	55
CD3 (%)	1	25[a]	0.4	76.3[a]
CD4 (%)	1	27[a]	0	5.3[a]
CD8 (%)	19b	16[b]	3.6[b]	34.4[b]
CD19 (%)	0	0	0.7	0.2
CD56 (%)	81	64	14.3	61.8

[a]Maternal origin
[b]NK cell origin

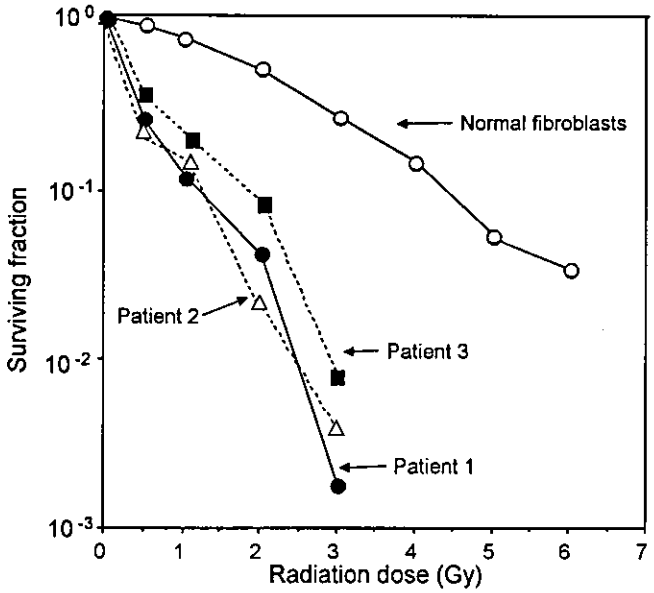

Fig. 1 Sensitivity of fibroblasts to irradiation. Primary fibroblasts obtained from the patients (*black circles* Patient 1, *open triangles* Patient 2, *black squares* Patient 3), and a normal control (*open circle*) lacking increased sensitivities to irradiation were cultured. The fraction of fibroblasts surviving after increasing doses (0.5–6 Gy) of γ-irradiation was determined. Results are expressed as survival relative to non-irradiated fibroblasts

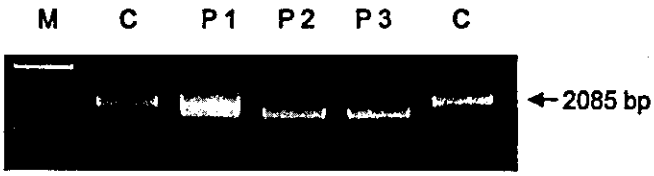

Fig. 2 Mutation analysis of *Artems* in Japanese RS-SCID patients (*M* standards). RT-PCR of *Artemis* mRNA transcripts in patient 1 (*P1*), patient 2 (*P2*), patient 3 (*P3*) and health controls (*C*)

product of Patient 1 is clearly shorter than the cDNA of normal controls; it forms a broad band that extends from approximately 1900 to 2085 bp. The size of the longest product is identical to that of healthy controls. The size difference between the shortest band and that of a healthy control suggests a deletion of approximately 100 bp. The sizes of the PCR products amplified from Patients 2 and 3 were also shorter in comparison with the normal controls and identical to the shorter product from Patient 1. Since we had difficulties in sequencing cDNA directly, we cloned the RT-PCR products obtained from RNA extracted from the fibroblasts of Patients 1 and 2. Sequence analysis of seven clones obtained from *Artemis* mRNA transcripts from Patient 1 showed one clone with exon 3 and exon 4 present, whereas the others lacked both exons 3 and 4. In Patient 2, all seven clones analyzed lacked both exons 3 and 4 (Table 2). On the other hand, both exons 3 and 4 were present in all clones obtained from the normal control. Moreover, we found the lack of exon 2 and/or exon 5 in some clones of both patients, suggesting alternative splicing.

To clarify the RT-PCR results, we performed direct long genomic PCR by using primers designed to amplify exons 2–4 of the *Artemis* gene in one piece and to screen for the presence or absence of exon 3 and exon 4. Two PCR products of different sizes were identified in Patient 1, his mother and brother (P1 B), whereas his father and a normal control had one product consisting of the longer band (Fig. 3A). Patient 2 had only the short product which was identical in size to the shorter band observed in Patient 1. The mother and father of Patient 2 demonstrated a heterozygous pattern, similar to that observed in the mother of patient 1, implying that both were carriers (Fig. 3B). Patient 3 had a single band of shorter size suggesting homozygosity, whereas patient 4 had a long and a short genomic PCR product (Fig. 3C).

To define the portion of the genomic deletion, we designed the nested PCR primer pairs located upstream and downstream of each exon. The extracted PCR product obtained from Patient 2 lacked exon 3 but contained exons 2 and 4 (Fig. 3D). Identical results were obtained from the single extracted product obtained from Patient 3 and the short product from Patients 1 and 4 (data not shown). Furthermore, we investigated the deletion site of exon 3 by the sequence analysis of "long" PCR products and found the deletion from 836 nucleotides upstream of exon 3 in the intron to nucleotides 4800 downstream of exon 3 in the intron in all patients (data not shown). These results demonstrated that Patient 2 and 3 were homozygous and Patients 1 and 4 were heterozygous for the genomic exon 3 deletion.

To identify the mutation affecting the second *Artemis* allele of Patient 1, we sequenced mRNA derived from clones with exons 3 and 4. We found an insertion of two nucleotides (AG) between 1205T and 1206G, whereas no insertion was found in that position in clones with exons 3 and 4 deleted (Fig. 4). The same AG insertion was found in one allele from the father of Patient 1 (data not shown). Both the genomic deletion of exon 3 and the 2-nt insertion

Table 2 Mutation of the *Artemis* gene of SCID patients in Japan (*nt* nucleotides, *FS* frame shift resulting in secondary termination)

Patients	Mutation	Effect	Status
P1	Deletion of exon 3	Exon 3 skipped	Heterozygous
–	2-nt insertion between T1205 and G1206	FS	Heterozygous
P2	Deletion of exon 3	Exon 3 skipped	Homozygous
P3	Deletion of exon 3	Exon 3 skipped	Homozygous
P4	Deletion of exon 3	Exon 3 skiped	Heterozygous
–	Unknown	–	–

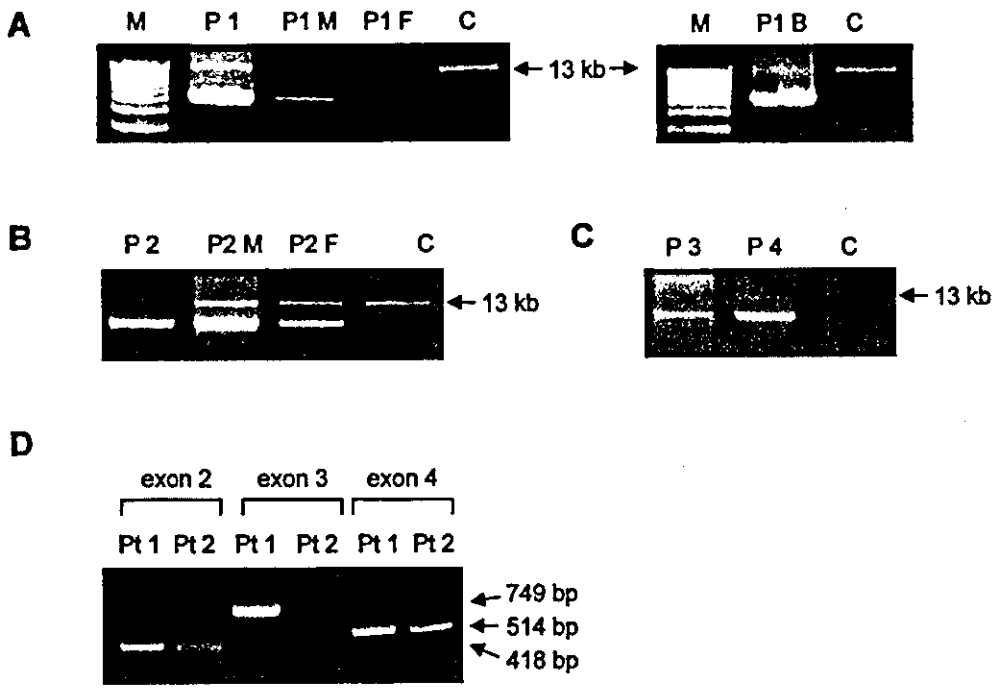

Fig. 3A–C "Long" PCR of genomic DNA with primers to amplify a region that includes exons 2–4 of the *Artemis* gene in **A** healthy controls (*C*), Patient 1 (*P1*), his mother (*P1 M*), his father (*P1 F*) and his brother (*P1 B*), **B** Patient 2 (*P2*), his mother (*P2 M*) and his father (*P2 F*), and **C** Patients 3 and 4 (*P3* and *P4*, respectively). **D** Nested PCR analysis of the "long" PCR product in Patient 1 (*Pt1*) and Patient 2 (*Pt2*). *M* Standards

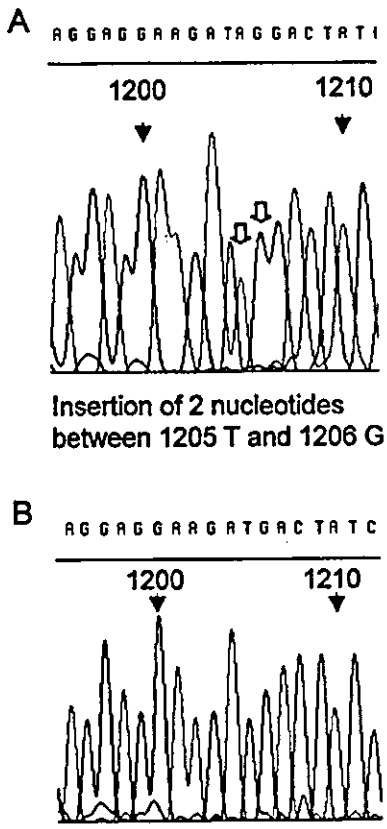

Fig. 4A, B Direct sequence of cDNA generated by RT-PCR of mRNA isolated from a clone with exons 3 and 4 obtained from Patient 1 (**A**) and a healthy control (**B**). The sequence adjacent to the mutation site is shown. A 2-nt insertion was found between 1205T and 1206G

in exon 14 of Patient 1 are novel mutations and, to date, only observed in this Japanese patient (Table 2).

Discussion

The four infants with T^-B^- SCID reported here are the first infants in east Asia identified to have RS-SCID attributable to a mutation of the *Artemis* gene. It is of interest that the four families, each with one affected infant, are unrelated and come from different parts of Japan. All four patients were found to have a genomic exon 3 deletion of the *Artemis* gene, two being homozygous and two heterozygous for this mutation. The second novel mutation, a 2-nt insertion in exon 14, was discovered in a single allele of one patient. Both mutations result in a frame shift and premature termination. This suggests that the genomic deletion of exon 3 represents a common mutation in the Japanese population.

Analysis of the RT-PCR product obtained from the exon 3 deleted *Artemis* gene revealed multiple splicing products, since all transcripts from alleles that had exon 3 deleted also lacked exon 4, and some transcripts had exon 2 and/or exon 5 deleted. Thus, the genomic deletion of exon 3 results in alternative splicing and the loss of adjacent exons. Interestingly, the unique nonsense mutation found in the 21 Athabascan-speaking native Americans also resulted in at least six alternatively splicing variants (Li et al. 2002). In contrast to the founder mutation of *Artemis* responsible for T^-B^- SCID in Athabascan-speaking native Americans (SCIDA) and the predominant genomic exon 3 deletion observed in Japanese population, the 13 patients from 11 unrelated families reported from Europe have a variety of mutations, including stop codons,

splice site mutations, nucleotide deletions, and several different genomic deletions (include deletion of exons 1–4, exons 5-6, and exons 5–8). As suggested by Moshous et al. (2000, 2001), the high incidence of genomic deletion is unique to the *Artemis* gene, suggesting a predisposition for gene deletion. To date, all mutations identified in the *Artemis* gene are complex or nonsense mutation, and amino acid substitutions have not been identified.

Two of our patients underwent successful bone marrow transplantation and are doing well following complete immunologic reconstitution. Since Artemis is expressed in almost all tissues and considered crucial for DNA repair, these immune reconstituted patients remain at risk for malignancies resulting from defective DNA repair mechanisms.

References

Cavazzana-Calvo M, Le Deist F, Saint Basile G de, Papadopoulo D, Villartay JP de, Fischer A (1993) Increased radiosensitivity of granulocyte macrophage colony-forming units and skin fibroblasts in human autosomal recessive severe combined immunodeficiency. J Clin Invest 91:1214–1218

Corneo B, Moshous D, Callebaut I, Chasseval R de, Fischer A, Villartay JP de (2000) Three-dimensional clustering of human *RAG2* gene mutations in severe combined immune deficiency. J Biol Chem 275:12672–12675

Li L, Moshous D, Zhou Y, Wang J, Xie G, Salido E, Hu D, Villartay JP de, Cowan MJ (2002) A founder mutation in Artemis, an SNM1-like protein, causes SCID in Athabascan-speaking native Americans. J Immunol 168:6323–6329

Ma Y, Pannicke U, Schwarz K, Lieber MR (2002) Hairpin opening and overhang processing by an Artemis/DNA-dependent protein kinase complex in nonhomologous end joining and V(D)J recombination. Cell 108:781–794

Moshous D, Li L, Chasseval R, Philippe N, Jabado N, Cowan MJ, Fischer A, Villartay JP de (2000) A new gene involved in DNA double-strand break repair and V(D)J recombination is located on human chromosome 10p. Hum Mol Genet 9:583–588

Moshous D, Callebaut I, Chasseval R de, Corneo B, Cavazzana-Calvo M, Le Deist F, Tezcan I, Sanal O, Bertrand Y, Philippe N, Fischer A, Villartay JP de (2001) Artemis, a novel DNA double-strand break repair/V(D)J recombination protein, is mutated in human severe combined immune deficiency. Cell 105:177–186

Schwarz K, Gauss GH, Ludwig L, Pannicke U, Li Z, Lindner D, Friedrich W, Seger RA, Hansen-Hagge TE, Desiderio S, Lieber MR, Bartram CR (1996) RAG mutations in human B cell-negative SCID. Science 274:97–99

Villa A, Sobacchi C, Notarangelo LD, Bozzi F, Abinun M, Abrahamsen TG, Arkwright PD, Baniyash M, Brooks EG, Conley ME, Cortes P, Duse M, Fasth A, Filipovich AM, Infante AJ, Jones A, Mazzolari E, Muller SM, Pasic S, Rechavi G, Sacco MG, Santagata S, Schroeder ML, Seger R, Strina D, Ugazio A, Valiaho J, Vihinen M, Vogler LB, Ochs H, Vezzoni P, Friedrich W, Schwarz K (2001) V(D)J recombination defects in lymphocytes due to RAG mutations: severe immunodeficiency with a spectrum of clinical presentations. Blood 97: 881–888

Hyper-IgM syndrome with putative dominant negative mutation in activation-induced cytidine deaminase

Yukiko Kasahara, MD, Hideo Kaneko, MD, PhD, Toshiyuki Fukao, MD, PhD, Tomoyoshi Terada, MD, PhD, Tsutomu Asano, MD, Kimiko Kasahara, and Naomi Kondo, MD, PhD *Gifu, Japan*

Background: Hyper-IgM immunodeficiency is an immunologic disorder characterized by normal or increased serum IgM levels and reduced serum IgG and IgA levels caused by the disruption of Ig class switching in B cells. The gene encoding activation-induced cytidine deaminase *(AID)* is responsible for the autosomal recessive form of hyper-IgM syndrome.

Objective: To investigate the relationship between the *AID* gene mutation and the clinical phenotype, we analyzed the *AID* gene in a female Japanese patient with the autosomal recessive form of hyper-IgM syndrome.

Methods: Genomic DNA and cDNA were extracted from neutrophils and analyzed by means of PCR. The *AID* gene was expressed as a glutathione S-transferase fusion protein. RT-PCR was performed after stimulation of the patient's PBMCs with phorbol myristate acetate and TGF-β.

Results: Despite significantly low serum IgG levels, our patient had not shown a predisposition to any severe infections, even without Ig replacement therapy. We identified a point mutation resulting in the stop codon in exon 5 of the *AID* gene (R190X) in the patient. No other mutations of the *AID* gene were detected in the patient. The same mutation was not detected in other members of her family. The mutant allele fused with the glutathione S-transferase protein was expressed stably at the same level as the normal allele. The *AID* gene expression in the patient was induced by phorbol myristate acetate and TGF-β.

Conclusion: The mutation of the *AID* gene is assumed to be of the dominant negative form. This is the first report of a dominant negative form of the mutation in vivo. (J Allergy Clin Immunol 2003;112:755-60.)

Key words: Hyper-IgM syndrome, activation-induced cytidine deaminase, dominant negative mutation

Hyper-IgM syndrome (HIGM) is a heterogeneous immunologic disorder characterized by normal or increased serum IgM levels and reduced serum IgG, IgA, and IgE levels.[1] The majority of affected patients have the X-linked form of the disease, which is due to the mutation of the CD40 ligand (HIGM1).[2-6] The CD40 ligand, a member of the TNF family, is expressed transiently on the surface of activated T cells.[7,8] Its receptor, CD40, is expressed on the surface of B cells.[9] The CD40-CD40 ligand interaction plays a critical role in isotype switching. The stimulation of B cells through the CD40 ligand in the presence of cytokines can induce the production of IgG, IgA, and IgE.[10,11]

Abbreviations used
AID: Activation-induced cytidine deaminase
CSR: Class switch recombination
GST: Glutathione S-transferase
HIGM: Hyper-IgM syndrome
PMA: Phorbol myristate acetate
SHM: Somatic hypermutation

Some patients with HIGM with autosomal recessive inheritance do not have defects in the CD40 ligand.[12-14] Ferrari et al[15] reported that mutations of the *CD40* gene cause an autosomal recessive form of immunodeficiency with hyper-IgM. Revy et al[16] have shown that some of these patients (HIGM2) have a mutation in a gene called activation-induced cytidine deaminase *(AID)*.

The AID protein has 198 amino acid proteins and was identified in 1999 by Muramatsu et al.[17] The human *AID* gene has been sequenced[18] and was mapped to chromosome 12p13. HIGM2 manifests itself as a defective class switch recombination (CSR), a defective somatic hypermutation (SHM), and hyperplastic lymphoid germinal centers.

Recently, several mutations in the *AID* gene have been identified. Revy et al[16] have identified 10 different types of mutation in the *AID* gene in 18 patients from 12 families. These mutations included amino acid substitutions, generation of premature stop codons, and deletions. Minegishi et al[19] have identified 3 different types of mutation in the *AID* gene in 18 patients. Most of these patients had homozygous point mutations or deletions in either exon 2, 3, or 4 among the 5 coding exons of the *AID* gene, resulting in missense mutations or stop codons.

Here we present the case of a patient with HIGM2 with the R190X mutation in the *AID* gene, which is assumed to be the dominant negative form of the *AID* gene.

From the Department of Pediatrics, Gifu University School of Medicine.
Received for publication March 18, 2003; revised June 9, 2003; accepted for publication June 9, 2003.
Reprint requests: Hideo Kaneko, MD, PhD, Department of Pediatrics, Gifu University School of Medicine, 40 Tsukasa-machi, Gifu 500-8705, Japan.

0091-6749/2003 $30.00 + 0
doi:10.1067/mai.2003.1708

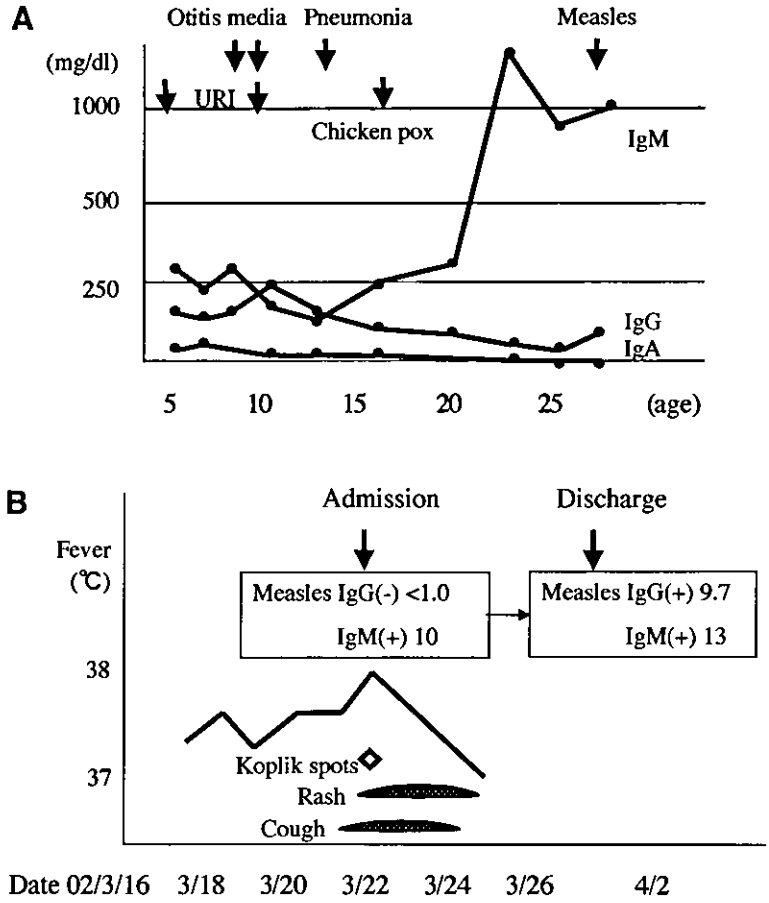

FIG 1. A, Clinical course and levels of serum Ig in the patient. With time, the serum IgG level gradually decreased, and the IgM level increased. She did not have severe infections, even without intravenous injection of Ig. **B,** Clinical course of the measles attack at 25 years old. The IgG level for measles increased 2 weeks later. *URI,* Upper respiratory tract infection.

METHODS

Sequencing

Genomic DNA from the Japanese female patient and her parents and brother were analyzed.[20] Informed consent was obtained from this patient and her family. The PCR conditions were 40 cycles at 94°C for 1 minute, 55°C for 1 minute, and 72°C for 1 minute. The primers for the 5 exons of the *AID* gene were as follows: exon 1, sense 5′-^{452}CATTAATTGAAGTGAGATTTTTCTGG-3′ and antisense 5′-^{720}TTGGGCTGACAGCGTATAAG-3′; exon 2, sense 5′-^{6213}GAAAATCCAGAGTGAGTGACCAG-3′ and antisense 5′-^{6590}TATGGGTGCATGGACATGGA-3′; exon 3, sense 5′-^{7711}GCATCCCCAAAGATCATTGC-3′ and antisense 5′-^{8161}GCTTCCCCACTAACTCATTCA-3′; exon 4, sense 5′-^{8321}TCTTCTACCCCCATATCCCC-3′ and antisense 5′-^{8600}CATCAGATGAAAACTGAGAGTG-3′; and exon 5, sense 5′-^{8921}CCATTCACTCAATTTGCTTC-3′ and antisense 5′-^{9060}CTGTCTTCAGCAGAGATATT-3′. PCR products were separated on a 1% agarose gel containing ethidium bromide and then sequenced.

Mutation detection

Genomic DNA samples from the patient and her parents and brother were amplified by means of PCR, the conditions of which were 40 cycles at 94°C for 1 minute, 55°C for 1 minute, and 72°C for 2 minutes. For concise detection of cC568T, we designed a mismatch primer introduced into the *Nde*I site in the mutant fragment: sense 5′-^{8958}CCTGTATGAGGTTGATGACATA-3′ and antisense 5′-^{9060}CTGTCTTCAGAGATATT-3′. The underlined A is a mismatch residue. The PCR fragments were electrophoresed on a 10% polyacrylamide gel after *Nde*I digestion.

Detection of expression of *AID* by means of RT-PCR

RNA was extracted from the patient's PBMCs and from control PBMCs, which were cultured in the presence or absence of 100 nmol/mL phorbol myristate acetate (PMA) and 1 ng/mL TGF-β.[21] The PCR conditions were 40 cycles at 94°C for 1 minute, 60°C for 1 minute, and 72°C for 1 minutes. The primers used were as follows: *AID*, sense 5′-^{49}GAGGCAAGAAGACACTCTGG-3′ and antisense 5′-^{695}GTGACATTCCTGGAAGTTGC-3′; β-actin, sense 5′-TGACGGGGTCACCCACACTGTGCCCATCTA-3′ and antisense 5′-CTAGAAGCATTTGCGGTGGACGATGGAGGG-3′. The PCR products were electrophoresed on 1% agarose gel and visualized by means of ethidium bromide staining.

Production of glutathione S-transferase fusion protein

AID cDNA was subcloned into the pGEX vector after PCR amplification and sequenced on both strands. *AID* cDNA was

expressed as a glutathione S-transferase (GST) fusion protein in *Escherichia coli* cells.

An isolated cDNA clone was inserted into the *Bam*HI site of a GST-tagged *E coli* expression vector (Pharmacia, Tokyo, Japan) to obtain a recombinant GST fusion protein, which was electrophoresed on a 10% SDS-PAGE for analysis.

RESULTS

The patient was 26 years old and had no family history of immunodeficiency or any other related diseases. The initial serum Ig levels were as follows: 270 mg/dL for IgG, 24 mg/dL for IgA, 135 mg/dL for IgM, and 3.2 IU/mL for IgE. With time, the serum IgG level gradually decreased, and the IgM level increased. Her current serum IgG level was 83 mg/dL, IgA level was less than 5 mg/dL, and IgM level was 1030 mg/dL (Fig 1, *A*). Her serum IgE level varied from 40 IU/mL to levels less than the detection limit. RAST revealed positivity for allergy to pollen, mite, and house dust. The serum Ig levels of the patient's father and mother were normal. CD40 and CD40 ligand were expressed normally in the patient's PBMCs. No mutations of CD40 or CD40 ligand that could lead to a loss of function were observed.[22] The patient had reduced percentages of circulating $CD4^+$ cells, although percentages of $CD3^+$, $CD8^+$, $CD19^+$, and $CD20^+$ cells were not reduced. The patient had repeated attacks of otitis media and upper respiratory tract infections since she was 2 years old. Although her serum IgG level was extremely low, she did not have severe infections. She had never received intravenous Ig therapy. She often had mild stomatitis and at 12 years old had atypical pneumonia, from which she recovered after the disease ran its natural course. Her antimycoplasma antibody level was not increased. When she was 25 years old, she had measles, although at the onset of the rash, she had negative IgG results for measles. However, 2 weeks later, she had positive IgG results for measles (Fig 1, *B*).

The *AID* gene was expressed in control unstimulated PBMCs (Fig 2). The stimulation of PBMCs with PMA and TGF-β resulted in the upregulation of *AID* gene expression. Moreover, the patient's unstimulated PBMCs weakly expressed the *AID* gene, and such expression was also upregulated by PMA and TGF-β (Fig 2).

Next we analyzed the *AID* gene in the patient. The cDNA sample of the patient showed a heterozygous mutation (Fig 3, *A* and *B*). The mutant cDNA showed a C-to-T substitution mutation at c568. This mutation resulted in a premature stop codon called R190X. There were no other mutations in the exons and exon-intron boundary of the patient's *AID* gene.

Genomic DNA from the patient demonstrated 2 peaks (Fig 3, *C*) corresponding to the N signal, including C (wild) and T (mutant) signals in exon 5, which indicates the heterozygous mutation of R190X. The sequences of genomic DNA of the *AID* gene from the patient's father, mother, and brother did not show any mutations.

We used mismatch primers, which were introduced artificially into the *Nde*I site. The mutant allele at cC568T was digested into 84- and 21-bp fragments by *Nde*I (Fig 4). The patient showed 2 bands corresponding to 105- and 84-bp band alleles. This indicates that the patient has both normal and mutant alleles. The patient's father, mother, and brother had only 105-bp wild-type fragments. R190X mutations were not detected in 200 normal alleles (data not shown). The wild-type and mutant AID proteins were produced as GST fusion proteins (Fig 5). The mutant AID protein was induced by isopropylthio-β-D-galactoside and was stable.

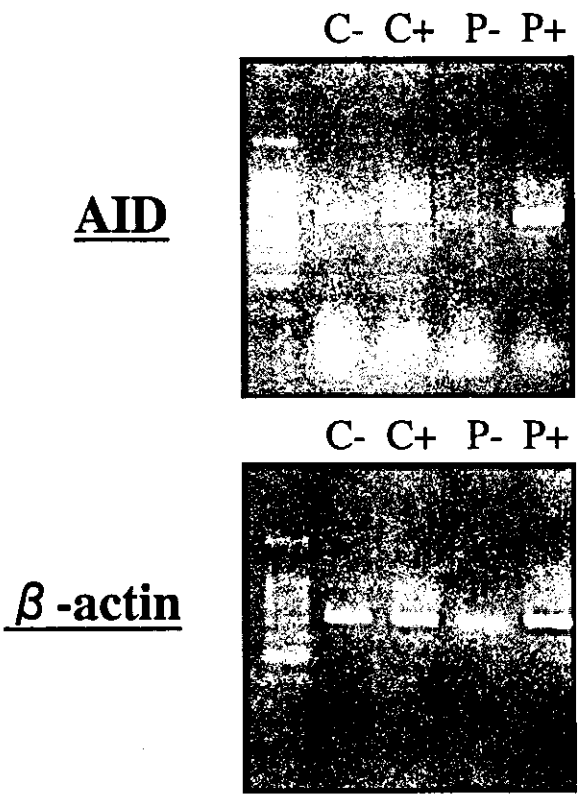

FIG 2. PCR analysis of expression of AID and β-actin in PMA- and TGF-β–stimulated PBMCs of the patient and control subject. The patient's *AID* gene expression was upregulated by PMA and TGF-β. *C–*, Control PBMCs without stimulation; *C+*, control PBMCs stimulated with PMA and TGF-β; *P–*, patient's PBMCs without stimulation; *P+*, patient's PBMCs stimulated with PMA and TGF-β.

DISCUSSION

We identified a heterozygous mutation of R190X in the *AID* gene of a patient with HIGM2. This mutation results in disorders of class switching and immunodeficiency.

Some studies have identified the *AID* gene as a candidate causative factor of HIGM2 on the basis of genetic screening and characterized the molecular defects in the *AID* gene in several patients. Most of the patients had homozygous point mutations or deletions in 3 of the 5 exons of the *AID* gene.[16,19] There have been no other reports describing the mutation of R190X observed in our patient. The patient did not have any mutations in other exons, although we did not determine the sequence of the promoter. In spite of the premature stop codon, the

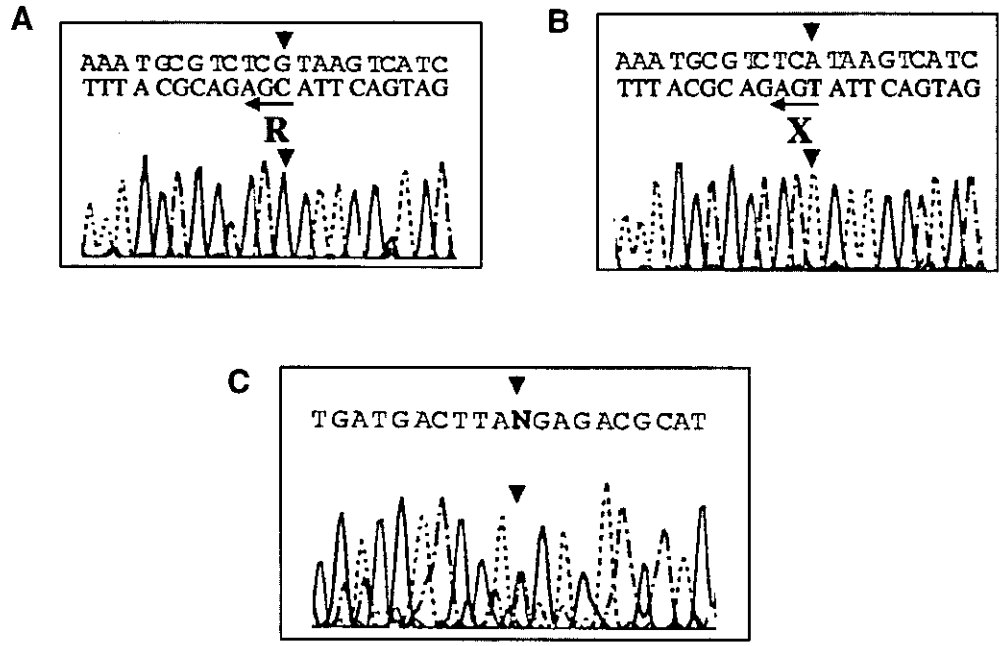

FIG 3. Sequence analysis of the *AID* gene (antisense patterns). Profiles of PCR products of cDNA (**A** and **B**) of the patient showed 2 patterns: wild-type and mutant. The mutant type (Fig 3, *B*) had a c568 C-to-T substitution *(arrow)*, resulting in the R190X mutation. The same region of genomic DNA (**C**) had an N peak consisting of C and T in exon 5 *(arrow)*. No other mutations were detected in the *AID* gene of the patient.

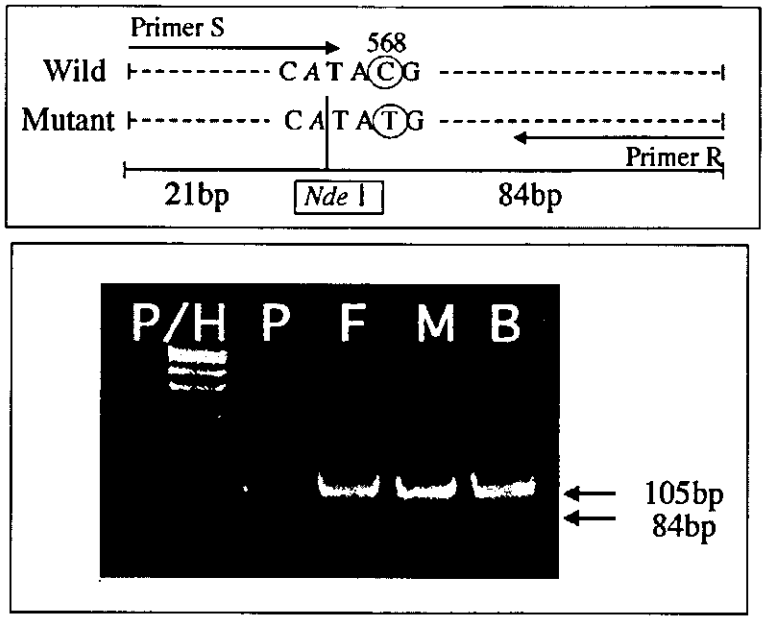

FIG 4. Detection of cC568T by using the artificial primer and *Nde*I digestion. As shown in the *upper panel*, the PCR product was 105 bp long (wild-type), and expected yields were 84- and 21-bp fragments (mutant) after *Nde*I digestion. *P/H*, Size marker; *P*, patient; *F*, patient's father; *M*, patient's mother; *B*, patient's brother.

mutant AID protein in the patient was stable as a GST fusion protein, as well as a wild-type protein.

The *AID* gene plays a crucial role in both CSR and SHM. The *AID* gene is produced and expressed only in germinal center B cells, which are CSR-SHM active.[17,23] Its expression is induced when mature B cells are activated to undergo CSR, SHM, or both. The *AID* gene is upregulated after stimulation of B cells with IL-4, TGF-β, and CD40 ligand.[17] In this study the *AID* gene of the patient was detected on the basis of TGF-β stimulation. These results demonstrate that the lymphocytes of the patient undergo the normal TGF-β signal cascade of response.

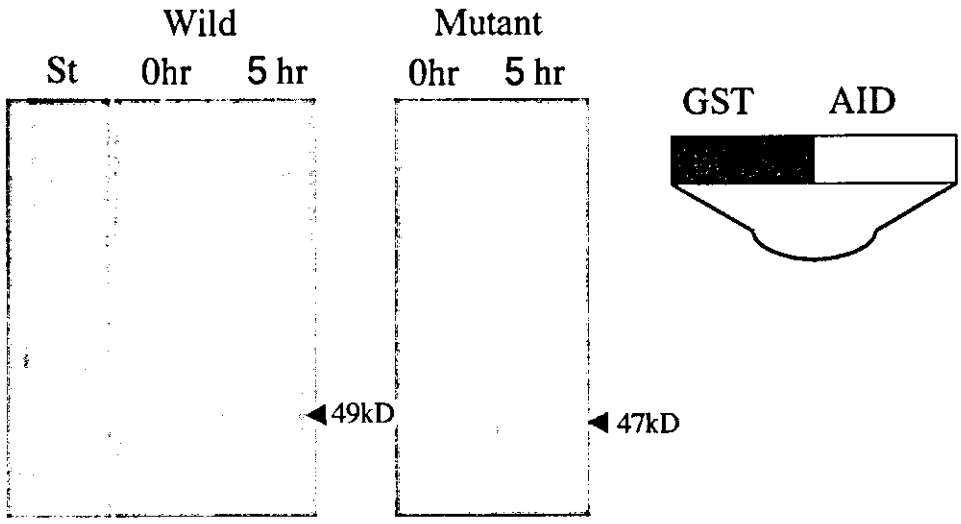

FIG 5. Expression of the GST-AID fusion protein. The mutant AID protein was 2 kd less than the wild-type AID protein because a carboxy terminus of 9 amino acids was deleted in the mutant AID protein. Both the wild-type and mutant were stably expressed as GST fusion proteins. *St*, Size marker.

It is interesting to note that the patient's IgG level for measles was increased 2 weeks after the onset of the rash, after which the IgG level for measles decreased (data not shown). This observation suggests that class switching occurs, but it is inadequate to maintain the acquired immunity in the dominant negative AID function. The patient had never been administered with intravenous Ig therapy, despite the low IgG level, because she had not had any severe infectious diseases. This mild infectious course without intravenous Ig therapy might be related to a dominant negative AID function. In this patient the expression of an intact *AID* gene might result in a mild phenotype for immunodeficiency.

The sequence of the *AID* gene is homologous to that of the mammalian RNA-editing deaminase, apoB mRNA-editing enzyme, catalytic polypeptide 1 which changes a single ribocytidine to uridine in the intestinal apolipoprotein-B mRNA.[24] The *AID* gene had deaminase activity when tested for deamination of deoxycytidine. Therefore the *AID* gene might be another RNA-editing deaminase. The mouse and human *AID* genes have 92% nucleotide sequence similarity. The alleles of c568C and 190 arginine are conserved between them.

Papavasiliou and Schatz[25] have generated a catalytic mutant protein by replacing amino acids at active sites of the *AID* gene in vitro (H56R/E58Q) and performed the deamination assay. Most cytidine deaminases act as homodimers or homotetramers. Therefore catalytic mutants exert a dominant negative effect on the deaminase activity.[26,27] The carboxy terminus is known to have a leucine-rich region and is considered to be important for apoB mRNA-editing enzyme, catalytic polypeptide 1 dimerization.[26] Furthermore, the algorithm model predicts the secondary structure of the carboxy terminus to be almost entirely α-helical, with a potential for coil formation.[28] The R190X mutation is not found on the predicted active site but at the carboxy terminus. The disorder of polymerization might be present and could cause immunodeficiency with hyper-IgM in our patient.

REFERENCES

1. Notarangelo LD, Duse M, Ugazio AG. Immunodeficiency with hyper-IgM (HIM). Immunodeficiency Rev 1992;3:101-21.
2. Allen RC, Armitage RJ, Conley ME, Rosenblatt H, Jenkins NA, Copeland NG, et al. CD40 ligand gene defects responsible for X-linked hyper-IgM syndrome. Science 1993;259:990-3.
3. Aruffo A, Farrington M, Hollenbaugh D, Li X, Milatovich A, Nonoyama S, et al. The CD40 ligand, gp39, is defective in activated T cells from patients with X-linked hyper-IgM syndrome. Cell 1993;72:291-300.
4. Korthauer U, Graf D, Mages HW, Briere F, Padayachee M, Malcolm S, et al. Defective expression of T-cell CD40 ligand causes X-linked immunodeficiency with hyper-IgM. Nature 1993;361:539-41.
5. DiSanto JP, Bonnefoy JY, Gauchat JF, Fischer A, de Saint Basile G. CD40 ligand mutations in X-linked immunodeficiency with hyper-IgM. Nature 1993;361:541-3.
6. Fuleihan R, Ramesh N, Loh R, Jabara H, Rosen RS, Chatila T, et al. Defective expression of the CD40 ligand in X chromosome-linked immunoglobulin deficiency with normal or elevated IgM. Proc Natl Acad Sci U S A 1993;90:2170-3.
7. Armitage RJ, Fanslow WC, Strockbine L, Sato TA, Clifford KN, Macduff BM, et al. Molecular and biological characterization of a murine ligand for CD40. Nature 1992;357:80-2.
8. Hollenbaugh D, Grosmaire LS, Kullas CD, Chalupny NJ, Braesch-Andersen S, Noelle RJ, et al. The human T cell antigen gp39, a member of the TNF gene family, is a ligand for the CD40 receptor: expression of a soluble form of gp39 with B cell co-stimulatory activity. EMBO J 1992;11:4313-21.
9. van Kooten C, Banchereau J. CD40-CD40 ligand. J Leukoc Biol 2000;67:2-17.
10. Briere F, Servet-Delprat C, Bridon JM, Saint-Remy JM, Banchereau J. Human interleukin 10 induces naive surface immunoglobulin D+(sIgD+) B cells to secrete IgG1 and IgG3. J Exp Med 1994;179:757-62.
11. Durandy A, Schiff C, Bonnefoy JY, Forveille M, Rousset F, Mazzei G, et

al. Induction by anti-CD40 antibody or soluble CD40 ligand and cytokines of IgG, IgA and IgE production by B cells from patients with X-linked hyper IgM syndrome. Eur J Immunol 1993;23:2294-9.
12. Conley ME, Larche M, Bonagura VR, Lawton AR 3rd, Buckley RH, Fu SM, et al. Hyper IgM syndrome associated with defective CD40-mediated B cell activation. J Clin Invest 1994;94:1404-9.
13. Callard RE, Smith SH, Herbert J, Morgan G, Padayachee M, Lederman S, et al. CD40 ligand (CD40L) expression and B cell function in agammaglobulinemia with normal or elevated levels of IgM (HIM). Comparison of X-linked, autosomal recessive, and non-X-linked forms of the disease, and obligate carriers. J Immunol 1994;153:3295-306.
14. Durandy A, Hivroz C, Mazerolles F, Schiff C, Bernard F, Jouanguy E, et al. Abnormal CD40-mediated activation pathway in B lymphocytes from patients with hyper-IgM syndrome and normal CD40 ligand expression. J Immunol 1997;158:2576-84.
15. Ferrari S, Giliani S, Insalaco A, Al-Ghonaium A, Soresina AR, Loubser M, et al. Mutations of CD40 gene cause an autosomal recessive form of immunodeficiency with hyper IgM. Proc Natl Acad Sci U S A 2001;98:12614-9.
16. Revy P, Muto T, Levy Y, Geissmann F, Plebani A, Sanal O, et al. Activation-induced cytidine deaminase (AID) deficiency causes the autosomal recessive form of the Hyper-IgM syndrome (HIGM2). Cell 2000;102:565-75.
17. Muramatsu M, Sankaranand VS, Anant S, Sugai M, Kinoshita K, Davidson NO, et al. Specific expression of activation-induced cytidine deaminase (AID), a novel member of the RNA-editing deaminase family in germinal center B cells. J Biol Chem 1999;274:18470-6.
18. Muto T, Muramatsu M, Taniwaki M, Kinoshita K, Honjo T. Isolation, tissue distribution, and chromosomal localization of the human activation-induced cytidine deaminase (AID) gene. Genomics 2000;68:85-8.
19. Minegishi Y, Lavoie A, Cunningham-Rundles C, Bedard PM, Hebert J, Cote L, et al. Mutations in activation-induced cytidine deaminase in patients with hyper IgM syndrome. Clin Immunol 2000;97:203-10.
20. Tashita H, Fukao T, Kaneko H, Teramoto T, Inoue R, Kasahara K, et al. Molecular basis of selective IgG2 deficiency. J Clin Invest 1998;101:677-81.
21. Kondo N, Inoue R, Kasahara K, Fukao T, Kaneko H, Tashita H, et al. Reduced expression of the interferon-gamma messenger RNA in IgG2 deficiency. Scand J Immunol 1997;45:227-30.
22. Kaneko H, Fukao T, Inoue R, Kasahara K, Matsui E, Kondo N. Long-term study of a female hyper-IgM immunodeficiency. Exp Clin Immunogenet 2000;17:173-8.
23. Longacre A, Storb U. A novel cytidine deaminase affects antibody diversity. Cell 2000;102:541-4.
24. MacGinnitie AJ, Anant S, Davidson NO. Mutagenesis of apobec-1, the catalytic subunit of the mammalian apolipoprotein B mRNA editing enzyme, reveals distinct domains that mediate cytosine nucleoside deaminase, RNA binding, and RNA editing activity. J Biol Chem 1995;270:14768-75.
25. Papavasiliou FN, Schatz DG. The activation-induced deaminase functions in a postcleavage step of the somatic hypermutation process. J Exp Med 2002;195:1193-8.
26. Oka K, Kobayashi K, Sullivan M, Martinez J, Teng BB, Ishimura-Oka K, et al. Tissue-specific inhibition of apolipoprotein B mRNA editing in the liver by adenovirus-mediated transfer of a dominant negative mutant APOBEC-1 leads to increased low density lipoprotein in mice. J Biol Chem 1997;272:1456-60.
27. Carlow DC, Carter CW Jr, Mejlhede N, Neuhard J, Wolfenden R. Cytidine deaminases from *B.subtilis* and *E.coli*: compensating effects of changing zinc coordination and quaternary structure. Biochemistry 1999;38:12258-65.
28. Kelley LA, MacCallum RM, Sternberg MJ. Enhanced genome annotation using structural profiles in the program 3D-PSSM. J Mol Biol 2000;299:499-520.

THE JOURNAL OF BIOLOGICAL CHEMISTRY
Vol. 278, No. 27, Issue of July 4, pp. 25234–25246, 2003
Printed in U.S.A.

Novel Human Homologues of p47^{phox} and p67^{phox} Participate in Activation of Superoxide-producing NADPH Oxidases*

Received for publication, December 17, 2002, and in revised form, April 9, 2003
Published, JBC Papers in Press, April 25, 2003, DOI 10.1074/jbc.M212856200

Ryu Takeya‡, Noriko Ueno‡, Keiichiro Kami‡, Masahiko Taura‡, Motoyuki Kohjima‡, Tomoko Izaki‡, Hiroyuki Nunoi§, and Hideki Sumimoto‡¶

From the ‡Medical Institute of Bioregulation, Kyushu University, 3-1-1 Maidashi, Higashi-ku, Fukuoka 812-8582, Japan and the §Department of Pediatrics, Miyazaki Medical College, Miyazaki 889-1692, Japan

The catalytic core of a superoxide-producing NADPH oxidase (Nox) in phagocytes is gp91^{phox}/Nox2, a membrane-integrated protein that forms a heterodimer with p22^{phox} to constitute flavocytochrome b_{558}. The cytochrome becomes activated by interacting with the adaptor proteins p47^{phox} and p67^{phox} as well as the small GTPase Rac. Here we describe the cloning of human cDNAs for novel proteins homologous to p47^{phox} and p67^{phox}, designated p41^{nox} and p51^{nox}, respectively; the former is encoded by NOXO1 (Nox organizer 1), and the latter is encoded by NOXA1 (Nox activator 1). The novel homologue p41^{nox} interacts with p22^{phox} via the two tandem SH3 domains, as does p47^{phox}. The protein p51^{nox} as well as p67^{phox} can form a complex with p47^{phox} and with p41^{nox} via the C-terminal SH3 domain and binds to GTP-bound Rac via the N-terminal domain containing four tetratricopeptide repeat motifs. These bindings seem to play important roles, since p47^{phox} and p67^{phox} activate the phagocyte oxidase via the same interactions. Indeed, p41^{nox} and p51^{nox} are capable of replacing the corresponding classical homologue in activation of gp91^{phox}. Nox1, a homologue of gp91^{phox}, also can be activated in cells, when it is coexpressed with p41^{nox} and p51^{nox}, with p41^{nox} and p67^{phox}, or with p47^{phox} and p51^{nox}; in the former two cases, Nox1 is partially activated without any stimulants added, suggesting that p41^{nox} is normally in an active state. Thus, the novel homologues p41^{nox} and p51^{nox} likely function together or in combination with a classical one, thereby activating the two Nox family oxidases.

Current attention has been increasingly paid to a gene family encoding superoxide-producing NAD(P)H oxidases, termed Nox[1] (1, 2). The mammalian members occur in various types of cells. The founder Nox protein gp91^{phox} (Nox2) is predominantly expressed in professional phagocytes such as neutrophils and plays a crucial role in host defense against microbial infection (3–9). On the other hand, Nox1 and Nox4 are abundant in epithelial cells in colon and kidney (10–14), respectively, but their biological roles are not well understood at present. The Nox oxidases are membrane-integrated proteins containing a complete electron-transferring apparatus (from NADPH to molecular oxygen) with binding sites for heme, FAD, and NADPH (3–9). In phagocytes, gp91^{phox} is complexed with p22^{phox} to form flavocytochrome b_{558}. The cytochrome is dormant in resting cells, but becomes activated during phagocytosis to generate superoxide, a precursor of microbicidal oxidants. The significance of the phagocyte oxidase in host defense is exemplified by recurrent and life-threatening infections that occur in patients with chronic granulomatous disease due to an impaired superoxide-producing activity of their phagocytes (9). On the other hand, the oxidase activity is strictly regulated, since inappropriate or excessive production of reactive oxygen species results in inflammatory disorders.

The activation of cytochrome b_{558} requires stimulus-induced membrane translocation of cytosolic proteins including the small GTPase Rac and the two specialized cytosolic proteins p67^{phox} and p47^{phox}, each containing two SH3 domains (3–9). In this process, p47^{phox} translocates to the membrane by itself, whereas p67^{phox} is recruited via p47^{phox} (15, 16); they constitutively associate via a tail-to-tail interaction (17–19). p47^{phox} binds via its SH3 domains to a proline-rich region (PRR) of p22^{phox}, the small subunit of cytochrome b_{558}; interaction plays a crucial role in the oxidase activation (20, 21). The SH3 domains are normally masked via an intramolecular interaction with the autoinhibitory region (AIR) that exists C-terminal to the domains (22). Upon cell stimulation, p47^{phox} becomes phosphorylated at multiple serines (23, 24), which induces a conformational change of this protein to render the domains in a state accessible to p22^{phox} (22, 25, 26). On the other hand, Rac is recruited upon cell simulation to the membrane independently of p47^{phox} or p67^{phox} (27). At the membrane, p67^{phox} directly interacts with GTP-bound Rac via the N-terminal domain that harbors four tetratricopeptide repeat (TPR) motifs (28, 29) and is thus targeted to cytochrome b_{558} (30–33), leading to superoxide production. Hence, the formation of the active phagocyte oxidase in cells requires the five proteins, namely gp91^{phox}, p22^{phox}, p67^{phox}, p47^{phox}, and Rac in the GTP-bound state; chronic granulomatous disease is caused by a defect of any of the genes encoding these proteins except Rac (9). The active oxidase can be formed in a cell-free system reconstituted with the purified proteins described above and anionic amphiphiles such as arachidonic acid (3–9). In the presence of excess amounts of p67^{phox} and Rac, however, p47^{phox} is not essential for the cell-free activation of the oxidase (33–35). It is thus

* This work was supported in part by grants-in-aid for Scientific Research and National Project on Protein Structural and Functional Analyses from the Ministry of Education, Culture, Sports, Science, and Technology of Japan, ONO Medical Research Foundation, and the BIRD project of JST Corp. The costs of publication of this article were defrayed in part by the payment of page charges. This article must therefore be hereby marked "*advertisement*" in accordance with 18 U.S.C. Section 1734 solely to indicate this fact.

The nucleotide sequence(s) reported in this paper has been submitted to the DDBJ/GenBank™/EBI Data Bank with accession number(s) AB097667 and AB095031.

¶ To whom correspondence should be addressed. Tel.: 81-92-642-6806; Fax: 81-92-642-6807; E-mail: hsumi@bioreg.kyushu-u.ac.jp.

[1] The abbreviations used are: Nox, NAD(P)H oxidase; NOXO1, Nox organizer 1; NOXA1, Nox activator 1; PRR, proline-rich region; AIR, autoinhibitory region; PB1, Phox and Bem 1; GST, glutathione *S*-transferase; MBP, maltose-binding protein; PMA, phorbol 12-myristate 13-acetate; SOD, superoxide dismutase; SH3, Src homology 3; EST, expressed sequence tag; CHO, Chinese hamster ovary; TPR, tetratricopeptide repeat; GTPγS, guanosine 5′-3-*O*-(thio)triphosphate.

considered that p67^{phox} is a protein that directly activates gp91^{phox} together with Rac, whereas p47^{phox} functions as an organizer in the activation.

In contrast to the phagocyte oxidase system, the activation mechanism for other members of the Nox family has remained largely unknown, except that Nox5 is shown to be activated by elevation of intracellular Ca^{2+} (36). Although it may be possible that Nox oxidases other than gp91^{phox}/Nox2 can also be regulated by p47^{phox} and p67^{phox}, this possibility has not been intensively tested. On the other hand, solely p47^{phox} or p67^{phox} exists in some types of cells containing one or more Nox oxidases, whereas neither p47^{phox} nor p67^{phox} is present in other types of Nox-expressing cells (37–39). In these cells, a heretofore unidentified protein possibly functions instead of p47^{phox} or p67^{phox} in activation of the phagocyte or other oxidases.

Here we describe the primary structure and function of novel human homologues of p47^{phox} and p67^{phox}. The novel proteins exhibit almost the same domain arrangement as the classical ones and can interact with the target proteins thus far identified for p47^{phox} or p67^{phox}, except that the p67^{phox} homologue fails to bind to p40^{phox}, a dispensable but significant regulator of the phagocyte oxidase (40). Consistent with these findings, the novel homologues are capable of supporting the activation of the phagocyte NADPH oxidase (*i.e.* gp91^{phox}). We also show that Nox1 becomes activated when it is coexpressed with both novel homologues of p47^{phox} and p67^{phox} or with a novel and a classical homologue.

EXPERIMENTAL PROCEDURES

Cloning of Human cDNAs Encoding Novel Proteins Homologous to p47^{phox} and p67^{phox}—A search of EST data bases with the C-terminal region of p47^{phox} yielded an EST clone encoding a protein homologous to p47^{phox} of 370 amino acids (GenBank™ accession number BC015917). Based on the sequences of these cDNA and genome DNA clones, we performed PCR using human multiple tissue cDNA panels (Clontech) and obtained a clone (GenBank™ accession number AB097667) that encodes the p47^{phox} homologue comprising 371 amino acids: Lys-49 of this cDNA clone is missing in the EST clone. The novel protein homologous to p47^{phox} was tentatively designated p41^{nox}, the gene of which is termed Nox organizer 1 (NOXO1; for details, see "Results").

We also performed a search of EST data bases with the C-terminal SH3 domain of human p67^{phox}, which yielded several cDNA clones containing partial sequences similar to those of p67^{phox}. Using the sequences, we further carried out the data base search to find several EST clones that encode N-terminal partial sequences of the protein homologous to p67^{phox}. Based on these partial sequences of these cDNA, we performed PCR using Human Multiple Tissue cDNA panels (Clontech) and obtained a cDNA clone encoding the full-length protein (GenBank™ accession number AB095031). The novel homologue of p67^{phox} was tentatively named p51^{nox}, the gene of which is termed Nox activator 1 (NOXA1; for details, see "Results").

Plasmid Construction—Complementary DNA fragments encoding various lengths of p47^{phox}, p67^{phox}, p40^{phox}, p22^{phox}, gp91^{phox}/Nox2, Nox1, Rac1, Rac2, and Cdc42 were prepared as previously described (13, 20, 22, 28). We also amplified the DNA fragments that encode p41^{nox}-F (amino acid residues 1–371), p41^{nox}-(SH3)$_2$ (residues 154–292), p41^{nox}-C (residues 293–371), p51^{nox}-F (residues 1–476), p51^{nox}-N (residues 1–224), and p51^{nox}-SH3 (residues 397–476) by PCR using specific primers from the cloned cDNAs encoding human p41^{nox} or p51^{nox}. The DNA fragments were ligated to the indicated expression vectors. Mutations leading to the indicated amino acid substitutions were introduced by PCR-mediated site-directed mutagenesis, and the mutated fragments were cloned into the indicated vectors. All of the constructs were sequenced to confirm their identities.

Two-hybrid Experiments—Various combinations between pGBT9 (Clontech) and pGADGH (Clontech) plasmids, each encoding an oxidase protein, were cotransformed into competent yeast HF7c cells containing a *HIS3* reporter gene, as previously described (28). Following the selection for Trp$^+$ and Leu$^+$ phenotypes, the transformants were tested for their ability to grow on plates lacking histidine, according to the manufacturer's recommendation (Clontech).

An in Vitro Binding Assay Using Purified Proteins—For expression in *Escherichia coli*, cDNA fragments were ligated to the following vectors: pGEX-2T (Amersham Biosciences) for glutathione *S*-transferase (GST) fusion protein; pMALc2 (New England Biolabs) for maltose-binding protein (MBP) fusion protein; or pProEX-HTb (Invitrogen) for His-tagged protein. GST-, MBP-, or His-tagged proteins were purified by glutathione-Sepharose-4B (Amersham Biosciences), amylose resin (New England Biolabs), or His-bind resin (Novagen), respectively, according to the manufacturers' protocols. For *in vitro* pull-down binding assays, a pair of a GST and an MBP fusion protein or a pair of a GST fusion and a His-tagged protein were mixed in 400 μl of phosphate-buffered saline (137 mM NaCl, 2.68 mM KCl, 8.1 mM Na_2HPO_4, and 1.47 mM KH_2PO_4) containing 10 mM dithiothreitol and incubated for 30 min at 4 °C. A slurry of glutathione-Sepharose-4B was subsequently added, followed by further incubation for 60 min at 4 °C. After washing four times with phosphate-buffered saline containing 0.5% Triton X-100 and 10 mM dithiothreitol, proteins were eluted from glutathione-Sepharose-4B with 10 mM glutathione in 100 mM Tris-HCl (pH 8.0) and 200 mM NaCl. The eluates were subjected to SDS-PAGE and stained with Coomassie Brilliant Blue or analyzed by immunoblot with an anti-His monoclonal antibody (Qiagen), followed by development using ECL-plus (Amersham Biosciences).

In Vivo Interaction between Oxidase Proteins—For expression of proteins in mammalian cells as HA- or Myc-tagged proteins, cDNAs were ligated to pEF-BOS (41), as previously described (42, 43). COS-7 cells transfected using LipofectAMINE (Invitrogen) with the indicated cDNA were cultured for 36 h and broken with a lysis buffer composed of 1% Nonidet P-40, 142.5 mM NaCl, 2 mM EDTA, 10% glycerol, leupeptin (40 μg/ml), aprotinin (10 μg/ml), 2 mM phenylmethylsulfonyl fluoride, and 20 mM HEPES, pH 7.4. Proteins of the lysate were precipitated with protein G-Sepharose using an anti-Myc monoclonal antibody (9E10; Roche Applied Science). The precipitants were analyzed by immunoblot with anti-HA or anti-Myc polyclonal antibodies (both from Santa Cruz Biotechnology.). The blots were developed using ECL-plus (Amersham Biosciences) to visualize the antibodies.

Activation of gp91^{phox} in K562 Cells—We transduced the gp91^{phox} gene into the leukemia cell line K562 and prepared cells that stably express a high amount of functional cytochrome b_{558} (K562-gp91^{phox} cells) as previously described (28). We also obtained a stable transformant expressing both p67^{phox} and gp91^{phox} (K562-gp91^{phox}/p67^{phox} cells) by further transducing the p67^{phox} gene to K562-gp91^{phox} cells, as previously described (22). The cDNA encoding the full-length of p41^{nox}, p51^{nox}, p47^{phox}, or p67^{phox} ligated to pEF-BOS was transfected by electroporation to K562-gp91^{phox} or K562-gp91^{phox}/p67^{phox} cells. The K562 cells (2×10^7 cells/ml) were electroporated in the presence of 20 μg of the plasmids at 170 V, 1070 microfarads using a Gene Pulser (Bio-Rad). Cells were cultured for 36 h and tested for superoxide-producing activity.

Superoxide production by the indicated cells was determined by superoxide dismutase (SOD)-inhibitable chemiluminescence with an enhancer-containing luminol-based detection system (DIOGENES; National Diagnostics), as previously described (22, 28). After the addition of the enhanced luminol-based substrate, the cells were stimulated with 200 ng/ml phorbol 12-myristate 13-acetate (PMA). The chemiluminescence was assayed using a luminometer (Auto Lumat LB953; EG&G Berthold).

Activation of gp91^{phox} and Nox1 in COS-7, HEK293, or CHO Cells—The cDNAs for gp91^{phox}/Nox2 and Nox1 (13) were ligated to the expression vector pcDNA3.0 (Invitrogen). The monkey kidney COS-7 cells or human embryonic kidney HEK293 cells were transfected using LipofectAMINE (Invitrogen) with the following combinations of cDNAs: pcDNA3.0-gp91^{phox}/Nox2 or pcDNA3.0-Nox1; pEF-BOS-p47^{phox} or pEF-BOS-p41^{nox}; and pEF-BOS-p67^{phox} or pEF-BOS-p51^{nox}. Although HEK293 cells lack Nox1 and gp91^{phox}, they express a small amount of Nox4 (13). However, Nox4 in HEK293 cells does not seem to affect the assay system; a weak superoxide-producing activity could be detected in a cell-free system composed of the membrane fraction of the cells and NAD(P)H, whereas no activity was observed at the cellular level, indicating that Nox4 in HEK293 cells produces superoxide within the cells but not outside of the cells (13). In some cases, the Chinese hamster ovary CHO cells were transfected with pEF-BOS-p41^{nox}, pEF-BOS-p51^{nox}, pEF-BOS-p22^{phox}, and pcDNA3.0-gp91^{phox}/Nox2 or pcDNA3.0-Nox1. After being cultured for 30 h, adherent cells were harvested by incubating with trypsin/EDTA for 1 min at 37 °C and washed with